Feature Article

Photochemistry of nanoporous carbons: Perspectives in energy conversion and environmental remediation

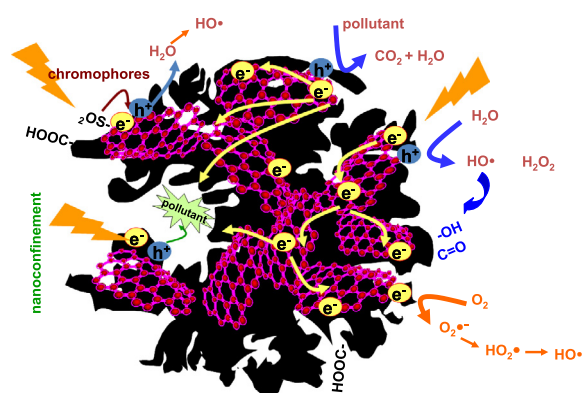Alicia Gomis-Berenguer [a], Leticia F. Velasco [b], Inmaculada Velo-Gala [a], Conchi O. Ania [a],*

[a] ADPOR Group, Instituto Nacional del Carbón (INCAR, CSIC), 33011 Oviedo, Spain
[b] Dept. Chemistry, Royal Military Academy, Renaissancelaan 30, 1000 Brussels, Belgium

GRAPHICAL ABSTRACT

ARTICLE INFO

ABSTRACT

The interest in the use of nanoporous carbon materials in applications related to energy conversion and storage, either as catalysts or additives, has grown over recent decades in various disciplines. Since the early studies reporting the benefits of the use of nanoporous carbons as inert supports of semiconductors and as electron acceptors that enhance the splitting of the photogenerated excitons, many researchers have investigated the key role of carbon matrices coupled to all types of photoactive materials. More recently, our group has demonstrated the ability of semiconductor-free nanoporous carbons to convert the absorbed photons into chemical reactions (i.e. oxidation of pollutants, water splitting, reduction of surface groups) opening new opportunities beyond conventional applications in light energy conversion. The aim of this paper is to review the recent progress on the application of nanoporous carbons in photochemistry using varied illumination conditions (UV, simulated solar light) and covering their role as additives to semiconductors as well as their use as photocatalysts in various fields, describing the photochemical quantum yield of nanoporous carbons for different reactions, and discussing the mechanisms postulated for the carbon/light interactions in confined pore spaces.

---

* Corresponding author.
  E-mail address: conchi.ania@incar.csic.es (C.O. Ania).

Contents

1. Introduction and background

The research related to light energy conversion and storage (particularly solar light) continues to be a topic at the forefront of technology that has attracted the attention of scientists across various disciplines. Photochemical reactions are particularly useful because the excitation of electronic molecular states using adequate energies may induce chemical bond breaking, offering interesting opportunities in environmental chemistry and energy production and conversion. In all these approaches, materials are used, as a few examples, for the conversion of light into electricity (via the photovoltaic effect), for energy production by the photoelectrochemical hydrogen generation or the photorreduction of CO$_2$ to produce fuels (light to chemical reactions), and to catalyze the degradation of environmental contaminants. Most commonly used materials in these processes are semiconductors (mainly Si and TiO$_2$) being their low photonic efficiency under sunlight a major technological drawback. Indeed, much of the incident radiation is usually wasted, as the photons with too small energy are not absorbed, while those with energy greater than the semiconductor band gap dispense of the excess by heating the material. As an example, the benchmark material, TiO$_2$, does not absorb photons with energy lower than 3.2 eV (that correspond to 387 nm), thus the sunlight exploitation is reduced to ca. 4%.

Numerous approaches have been established for overcoming this limitation, mostly focusing on the development of new materials with improved harvesting features across the visible region (organic metal halides, perovskites, transition metal oxides and sulfides, non noble metal-based catalysts) [1–5]. For instance, many efforts have concentrated in the synthesis of novel semiconductors with narrow bandgaps (e.g., WO$_3$, Bi$_2$WO$_6$) [6,7], the incorporation of metallic dopants or other impurities to induce modifications in the electronic band structure associated to band gap narrowing and localized midgap energy levels [8–18], surface sensitization [19,20], the use of hybrid nanostructured photocatalysts [21], or the coupling of catalysts with narrower (direct) band gap semiconductors [22,23], among most representative. Another alternatives are based on porous photocatalysts and/or the immobilization of the photoactive material on porous substrates (mainly zeolites, silica, activated carbons); in these cases, the enhanced response has been explained in terms of the increased mass transfer rate of the pollutant from the bulk solution to the catalyst's surface provided by the porosity, causing a better contact of the pollutant with the active sites of the photocatalyst [24,25].

Extensive work has also been carried out on the use of carbon materials for this purpose; many researchers have sought to couple different forms of carbons with TiO$_2$ and other semiconductors for enhancing the spectral response in the UV and visible light range [26–32]. The first studies on the use of activated carbons relied on the confinement of the pollutant in the porosity of the carbon (considered as an inert support) coupled with the photoactivity of the semiconductor [26,30]. Since then, a variety of carbon sources, forms and morphologies have been explored using conventional and novel carbons as additives and supports.

Among all forms of carbons, graphene has been extensively investigated as additive to semiconductors owing to its unique physical, chemical, optical and electronic properties that seemed to offer promising routes towards its light energy conversion ability [33–37]. Despite of the singular features of graphene, some authors raised the concern on its use for photocatalytic purposes manifesting that TiO$_2$/graphene composites are in essence the same as other TiO$_2$/carbon composite materials on enhancing the photocatalytic activity of TiO$_2$ [35].

It seems generally accepted that the role of the carbon material differs for porous carbons (activated carbons, carbon fibers and nanofibers, carbon foams and so forth) compared to other forms of nanostructured carbons (carbon nanotubes, fullerenes and graphene) due to their different structural properties. For instance, for carbons with high electron mobility the superior response of semiconductor/carbon photocatalysts has been associated to the strong interfacial electronic effects between the carbon phase and the photocatalyst, that favor the separation of the photogenerated carriers through its stabilization in the π electron density of the carbon (acting as sinks of electrons), and to the role of carbon as photosensitizer (as effective photosensitizers typically present high densities of C=C double bonds) [31,32,38,39]. In the case of nanoporous carbons, the enhanced photoactivity of carbon/titania composites has been traditionally discussed mainly in terms of the above-mentioned enhanced mass transfer of the adsorbed pollutant from the bulk solution and the interactions between the carbon support and the immobilized catalyst [30,40,41].

By that time, our research group reported the first experimental evidence on the photochemical activity of nanoporous carbons under UV–visible irradiation in the absence of semiconductors [42,43], as well as their ability to generate reactive radical species when exposed to light in aqueous environments [44,45]. Amazingly, despite the close similarities between the structural and chemical features of nanoporous carbons and those of graphene, yet the photochemical activity of this old form of carbons had been neglected and disregarded. Since then, we have investigated the application of nanoporous carbons in photochemical reactions under varied irradiation conditions, the dependence on the surface

chemistry of the carbon matrix, the wavelength of the irradiation source, and the performance towards different photoassisted reactions [44–50].

The aim of this paper is to provide an overview on the possibilities of exploiting the interactions of nanoporous carbons and different sources of irradiation (UV, simulated solar light) in different fields of research, covering the progress in the photocatalytic degradation of pollutants using semiconductor/carbon and nanoporous carbons as catalysts (where advanced oxidation processes based on carbon materials may be coupled to highly skilled adsorption technologies for air purification and water remediation), as well as the new perspectives on the use of nanoporous carbons as photoanodes in the water photooxidation reaction, and in photorreduction reactions.

2. Nanoporous carbons as additives to semiconductors

After the pioneering works in 1960s and 70s reporting the photocatalytic activity of ZnO and TiO$_2$ electrodes [51,52], the interest of semiconductor photocatalysis has growth, particularly in the fields of energy conversion/storage and environmental remediation. Traditionally, heterogeneous photocatalysis has been associated to the use of inorganic semiconductors as photoactive materials; TiO$_2$ is the benchmark material due to its low cost, large availability, chemical inertness, low toxicity and stability against photo- and chemical corrosion, but many other transition metal oxides and sulfides such as ZnO, CdS, ZnS, WO$_3$ have been also widely investigated [7,53–56].

The mechanism of light absorption in a wide band gap *n*-type semiconductor - such as titanium oxide - is based on interband electron transitions. Briefly, when the semiconductor particles are irradiated with photons with energy equal to or higher than its band gap, electrons are excited from the valence band to the unoccupied conduction band, whereas holes (vacancies) are created in the valence band. The photogenerated charge carriers (electron/hole pairs) can recombine (emitting light or dissipating the energy as heat), or migrate to the surface to react with electron donors or acceptors. The competition between these processes determines the efficiency of the photocatalytic reaction; for environmental applications, the efficiency is also often measured as the rate of generation of reactive radical species (mainly HO$^\cdot$ and O$_2^-\cdot$). The redox potential of the photogenerated holes in TiO$_2$ is 2.53 V vs standard hydrogen electrode (SHE) [52,57], positive enough to directly oxidize the pollutant, and/or to react with water molecules or hydroxyl groups to produce HO$^\cdot$, which is also a powerful oxidizing agent (2.81 V vs SHE). Similarly, the redox potential of the conduction band electrons is −0.52 V vs SHE, negative enough to form O$_2^-\cdot$ (0.89 V vs SHE) or H$_2$O$_2$ (1.78 V vs SHE) when oxygen is present in the medium. All these species can undergo further decomposition reactions, enhancing the efficiency of the overall photocatalytic process. Hence, the edges of the conduction and valence bands must have potentials more negative and more positive than the potentials of the O$_2$ and HO$^\cdot$/OH$^-$ couples, respectively, which has been shown not to be the case for some semiconductors (i.e., WO$_3$).

Triggered by the low photonic efficiency of most photocatalysts under sunlight, numerous efforts have been made in the last decades to improve the optical properties of semiconductor materials. Photocatalyst band-gap tuning via chemical modification, doping of the semiconductor lattice for reducing surface recombination, synthesis of nanosized catalysts for an efficient charge separation, and increasing the crystallinity, are among most representative [57–64]. The use of carbon either as dopant of semiconductors into their crystalline structure or as additive has appeared as an interesting alternative to attain high photoconversion efficiencies. To illustrate this issue, in the following sections we discuss the role of nanoporous carbon materials of varied nature and structure as additives to various semiconductors – i.e., TiO$_2$, WO$_3$ and Bi$_2$WO$_6$– for their application in the photodegradation of pollutants and the photoelectrochemical oxidation of water for energy conversion.

2.1. TiO$_2$/Nanoporous carbon

TiO$_2$ is the most commonly used photocatalyst under UV light [65]; however, its limited efficiency under sunlight irradiation, and the operation problems related to the recovery and re-use of the catalyst, associated to nano-sized titania powders make its large-scale implementation a difficult task. The use of supports is intended to overcome this issue [66]. In this regard, the photocatalytic response of carbon/TiO$_2$ composites has been widely explored for a variety of carbon sources, forms and morphologies using different synthetic routes. Indeed, many studies have focused on the synthesis and performance of TiO$_2$/carbon photocatalysts using various carbon and titania precursors, as well as varied methods for the incorporation of the carbon component to the catalyst (e.g., mechanical mixture, coating by liquid impregnation, hydrothermal process, chemical vapor deposition) [66–68]. The enhanced photoactivity of carbon/titania composites has been discussed by different mechanisms, depending on the nature of the carbon matrix itself. In the case of nanoporous carbons, it has been typically ascribed to the enhanced mass transfer of the adsorbed pollutant from the bulk solution to the photoactive TiO$_2$ particles through the interface between the two catalyst components, and to the interactions between the inert substrate and the immobilized catalyst [69–71]. This is important because the reaction takes place essentially at the catalyst/water interface, particularly if radical species are involved since these reactive species do not migrate far from the photoactive sites where they are generated [71]. Moreover, the use of porous carbon supports also contributes to a faster sedimentation and an easier recovery of the photocatalyst from the reaction medium, allowing to perform cycles and hence favoring an eventual integration in large-scale photocatalytic systems [70].

To account for the effect of the carbon support in the performance of TiO$_2$/carbon catalysts, a synergistic factor has been defined as the ratio between the apparent rate constants of the photoconversion reactions corresponding to the supported and bare titania catalysts [30]. This factor, however, does not account for some other operating parameters (photoreactor geometry, illumination source, mass-transfer limitations, diffusion or convection control, chemical structure of the pollutant, temperature, etc.) that control the reaction rate and yield, for which comparison of catalysts in different experimental conditions must be done carefully.

The presence of the carbon component in TiO$_2$/carbon photocatalysts has also been reported to modify the degradation route of organic pollutants boosting the degradation of the intermediates - as they are formed nearby the photoactive sites of the TiO$_2$/carbon catalysts-, with some studies reporting the faster mineralization degrees and higher removal efficiencies [26,42,67–74]. For instance, using carbons of various origins we observed the regioselective oxidation of phenol to form *ortho*-dihydroxylated intermediates with TiO$_2$/carbon photocatalysts [75,76], indicating that in the presence of the carbon additive the oxidation proceeds through the electrophilic attack of the aromatic ring, which is a more advantageous degradation route for the complete mineralization of this pollutant as it proceeds through a less number of subproducts [77]. The modification of the photooxidation pathway of organic pollutants has been explained by the occurrence of weak interactions between the carbon and the semiconductor surfaces, as evidenced by infrared spectroscopy and the distribution of the catalyst surface charges in solution [70,76].
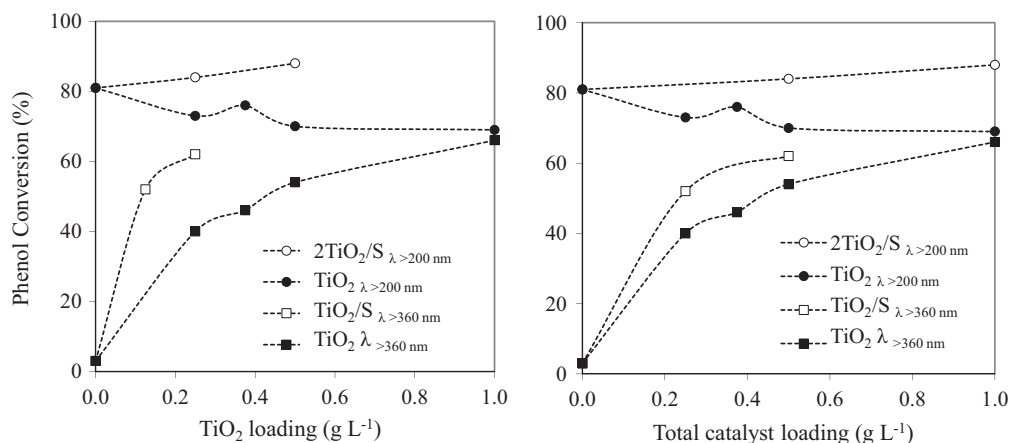
Fig. 1. Effect of the irradiation wavelength on the conversion of phenol in TiO_2 and TiO_2/carbon photocatalysts (S stands for a sisal rope-derived nanoporous carbon) for various (a) TiO_2 loadings and (b) total catalyst loading (symbols represent experimental values while lines are guides for the eye). Initial concentration of phenol of 86 mg/L. Reprinted from Ref. [75], copyright 2015, with permission from Elsevier.

The degradation mechanism is also influenced by the wavelength irradiation source [75]. A series of experiments performed using polychromatic light and filters to cut-off the irradiation below 360 nm (lamps emitting at $200 > \lambda > 600$ nm and $\lambda > 360$ nm) showed increased photoconversion values for TiO_2/-carbon catalysts (1:1 wt ratio) using high energy photons; the breakdown of the intermediates and the regioselectivity towards the *ortho*-substitution was also higher when the catalyst was exposed to light at $200 > \lambda > 600$ nm (Fig. 1).

The method for the immobilization of TiO_2 on the carbon support is also important as it may control the photocatalytic activity by defining the recombination lifetime and interfacial interactions between the two phases (i.e., inducing crystal defects or modifying the surface morphology of the catalyst) [26,66,72,78,79]. Interesting titania/carbon photocatalysts with improved photocatalytic activity and showing controlled morphology and topology of the active phase (core-shell, shell-core, carbon coating) have been prepared using hydrothermal carbonization methods [74,80] and coating procedures [81–84]. However, when nanostructured carbons with high electron mobility are used as additives (i.e., carbon nanotubes), the electronic structure and structural defects of the carbon material seem to be much more important than its chemical composition or any chemical bond between carbon and TiO_2 [85].

The porosity of the carbon support is also important; an eventual blockage of the porosity of the carbon support by the semiconductor nanoparticles would limit the adsorption of the pollutant in the (micro) porosity of the carbon, counteracting the beneficial effect of the carbon additive [72]. On the other hand, if the porosity remains accessible during the photocatalytic runs, the overall photodegradation yield is enhanced [76]. Although large surface areas and pore volumes are usually required in the carbon additive for obtaining a high dispersion of the semiconductor, they are not essential to achieve high degradation rates and efficiencies. Related to this, a carbon foam (CF) with an open porous structure was used as support of titanium oxide for the photocatalytic degradation of phenol [86], and the composite showed better results in terms of degradation rate than nonsupported titania, comparable to those of other TiO_2/nanoporous carbon composites. Considering the less developed porous features of this photocatalyst compared to other TiO_2/nanoporous carbons (i.e., surface areas of 165 vs 924 m^2/g), it was concluded that rather than a well-developed microporosity, the key factor for an optimal photocatalytic performance is to provide an accessible pore structure that avoids any diffusion

restrictions for the accessibility of the pollutant from the bulk solution to the support/titania.

Further insights on the mechanisms occurring at the TiO_2/carbon interface were obtained by investigating the optoelectronic and photoelectrochemical response of carbon/titania electrodes of increasing carbon content ranging from 5 to 50 wt.% during repeated on/off cycles of illumination [87]. The shape of the current-potential curves of the carbon/titania electrodes was similar to that of a titania electrode, merging the characteristic fingerprint of *n*-type semiconductor with the capacitive contribution due to the porosity of the carbon material. Upon illumination, anodic photocurrents were recorded in the electrodes, when the bias potential was positive enough for an efficient hole-electron separation. The photocurrent responses were rapid and reproducible, retracting to their original values almost instantaneously once the illumination was turned-off. Interestingly, similar photocurrent values were obtained for the carbon/titania and TiO_2 electrodes, despite the amount of semiconductor was gradually decreasing. The high photocurrents measured in the carbon/titania electrodes were related to a higher density of photogenerated electrons recovered at the back contact of the electrical circuit, suggesting a more efficient charge carrier separation at the electrode/electrolyte interface upon the incorporation of the carbon additive. Two mechanisms were postulated to describe the role of the carbon component in the enhanced response of the titania/carbon electrodes: (i) a more efficient charge carrier separation due to the smaller diffusion length through the nanoporosity of the carbon additive; (ii) the role of the carbon matrix as an acceptor of the photogenerated electrons, boosting the separation of the charge carriers through delocalization and stabilization within the graphene-like layers of the carbon additive. Additionally, the studied nanoporous carbon showed an important selfphotoactivity upon irradiation, thus a third mechanism considering the photon absorption by the carbon material itself due to various electronic transitions was proposed. This issue will be further addressed in a different section.

Inspired on the extensive literature on metallic TiO_2 doping with reported visible light activation of the doped catalyst due to the effective electronic interaction between the semiconductor and the metal [88–91], we explored a novel approach based on adding the metallic dopant to the carbon [92]. Copper was selected as it is an effective dopant for trapping the electrons in the conduction band of TiO_2 and catalyzes many oxidative reactions [91,93,94]. However, as many other metal-doped semiconductors, it suffers from deactivation due to aggregation of the metallic

dopants [95]. The titania/copper-doped carbon catalysts displayed good degradation yields for the elimination of phenol under visible light (in terms of conversion, regioselectivity in the formation of intermediates, superior mineralization degree and enhanced degradation rate), due to the homogeneous dispersion of copper particles (predominantly copper (II) species) within the carbonaceous matrix [92]. The effect of copper was attributed to its role as oxygen activator and/or the fast electron transfer environment, which would minimize the recombination of the excited electron-/hole pairs created upon illumination of the semiconductor [92,96]. For instance, the photoexcitation of the semiconductor near the Cu (II) species can lead to the formation of O-radicals under visible light irradiation, to produce Cu(I) intermediates [92]. The reduced metal species would interact with dissolved O_2 adsorbed in the hydrophobic sites of the carbon, regenerating the Cu(II) and further radical species responsible for the improved photooxidation [92].

In sum, the use of nanoporous carbons as additives to titania powders is an interesting alternative to improve the conversion efficiency of the semiconductor. The versatility and availability of carbons with varied pore architectures and composition (coupling metal doping and surface modification to pore control) offer unlimited possibilities particularly in the environmental remediation arena. The adequate choice of the carbon additive may overcome the low photonic yield of TiO_2 under sunlight (due to superior light absorption features of the TiO_2/carbon composites) as well as increasing the overall efficiency in terms of mineralization by tuning the degradation mechanisms via "regioselective reactions".

2.2. Bi₂WO₆/nanoporous carbon

Bismuth-based materials are being widely investigated as alternatives to TiO_2 in photocatalytic applications. Among them, Bi_2WO_6 with a layered structure with perovskite-like slabs of WO_6 and $[Bi_2O_2]^{2+}$ layers, has shown good light absorption properties under visible light irradiation, offering interesting perspectives in sunlight-driven photocatalysis [97–100]. The physical characteristics of Bi_2WO_6 (surface area, morphology, particle size, crystallinity) can be strongly affected by the synthesis method; this material also displays a weak stability during long illumination periods [98,99]. Both aspects constitute a major drawback for the application of Bi_2WO_6 in photocatalytic processes. In this regard, the superior photocatalytic activity of Bi_2WO_6/carbon composites has been reported for various carbon additives - activated carbons [101], glucose-derived carbons [102,103], carbon quantum dots [104] or carbon nanotubes [105] - and nominal carbon contents (between 0.5 and 25 wt.%). In our study we explored the use of Bi_2WO_6/carbon photocatalysts for the degradation of rhodamine B (RhB) under simulated solar light, using carbon materials of different physicochemical properties (Fig. 2) [105]. The photocatalysts were prepared following two different synthetics approaches: (i) physical mixing of the carbon additive and the semiconductor and (ii) through a one-pot route consisting on allowing the synthesis of the semiconductor in the presence of the carbon material. Our results demonstrated the critical role of the synthetic route followed to incorporate the carbon additive to a semiconductor so as to obtain an effective interface between both phases.

Due to the non negligible adsorption capacity of the Bi_2WO_6/carbon composites (i.e., $S_{BET} < 50$ m²/g), the photocatalytic runs were carried out on preloaded catalysts under darkness. Based on the photocatalytic results, it was established that the performance of the Bi_2WO_6/carbon photocatalysts did not depend exclusively on the porous features of the carbon additive (although porosity is important); the synthetic route followed for the preparation of the composites had also an important effect. For instance, the conversion of RhB was faster for the catalysts prepared by incorporating the carbon additive during the synthesis of the semiconductor, than for those obtained by physical mixture (with conversions below those of the semiconductor alone). This was attributed to the proper contact between the carbon phase and the semiconductor particles in the one-pot synthesis. Indeed, performing the synthesis of the semiconductor in the presence of small amounts of
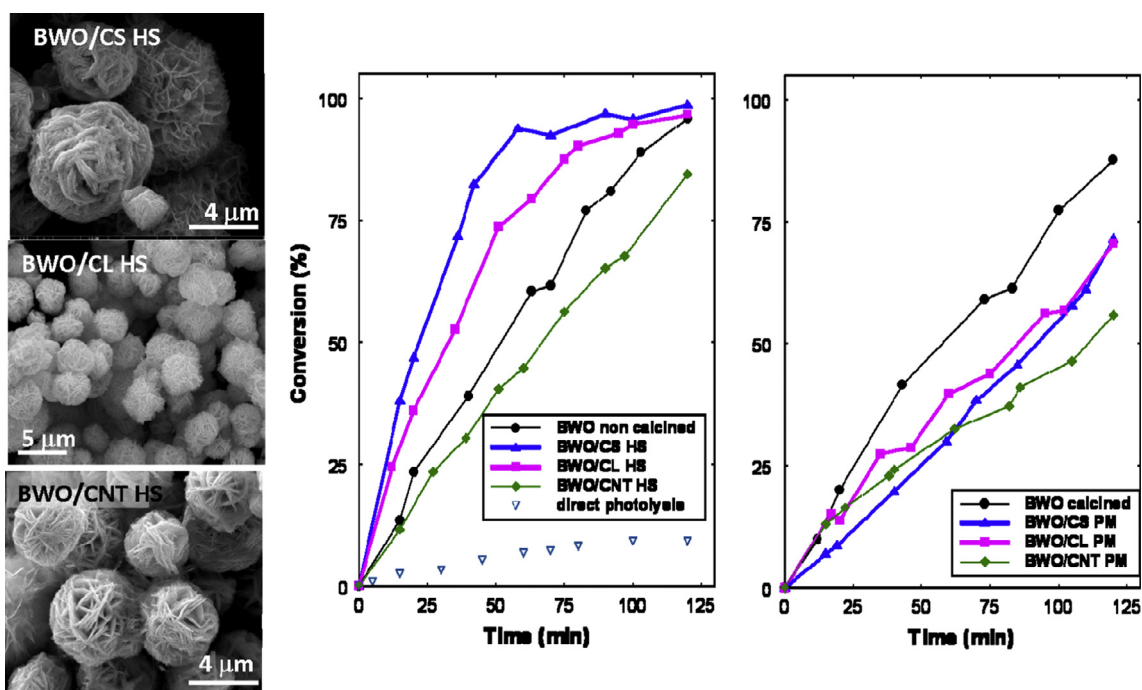
Fig. 2. Conversion of rhodamine B using simulated solar light and Bi_2WO_6/carbon photocatalysts prepared by physical mixing of the semiconductor and nanoporous carbon powders (series PM) and synthesizing the semiconductor in the presence of the carbon additive (series HS). SEM images of selected BWO/carbon mixtures of the HS series. Adapted from Ref. [105], copyright 2015, with permission from Elsevier.
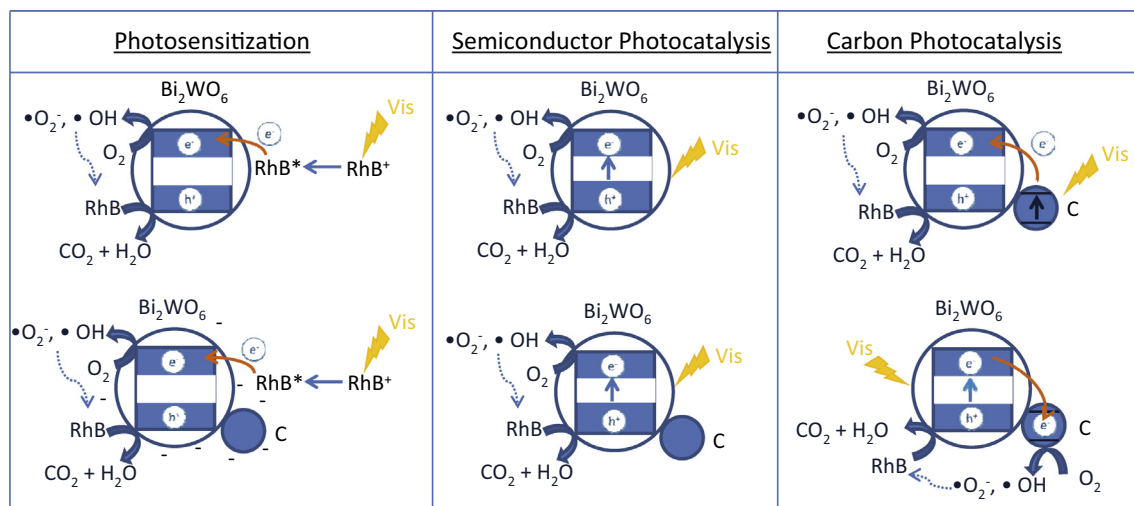
Fig. 3. Schematic representation of the different degradation routes of rhodamine B in the presence of Bi_2WO_6 and Bi_2WO_6/carbon photocatalysts. Reprinted from Ref. [105], copyright 2015, with permission from Elsevier.

carbon additive (ca. 2 wt.%) did not affect the assembling semiconductor particles (neither morphology or crystallinity), that displayed the same flower-like morphology of Bi_2WO_6 with slightly smaller particle sizes. On the other hand, the preparation of the catalysts by physical mixing led to uneven distributions of the carbon additive in the final composite. This was more evident in the case of carbon nanotubes, showing that using a carbon additive with high electron mobility does not grant a superior photocatalytic performance of the composite.

The shielding effect of the carbon matrix and the surface acidity of the photocatalysts on their photocatalytic performance were also noticed, with the highest conversions of RhB obtained for acidic photocatalysts. The dependence of RhB degradation on the surface basicity/acidity of the catalyst has also been reported for other semiconductors, and attributed to coupled independent mechanisms that can proceed side by side (photosensitization, photocatalysis and carbon-photon mediated reactions) [105–107]. Indeed, RhB is an amphoteric dye with a permanent positive charge (diethylamino group) and a negative charge upon dissociation of the carboxylic moiety, thus the interactions with the catalysts surface depend on its ionization state. In our experimental conditions the zwitterionic form of RhB (positively charged) is predominant in solution [108,109], for which strong interactions are favored in catalysts of acidic nature.

Based on the conversion and high mineralization values, the photodegradation of RhB in the Bi_2WO_6/carbon composites proceeded through several simultaneous mechanisms (Fig. 3). When using acidic carbon additives, the resulting Bi_2WO_6/carbon composites were negatively charged, thus RhB is preferentially adsorbed by the diethylamino group (positively charged) and the degradation occurs via the successive ethylation of the alkylamine moiety [101,110]. The strict requirements needed for the N-ethylation process (i.e., formation of the excited state of the dye and transfer of electrons from the dye to the conduction band of the semiconductor) pointed out the good chemical contact between the catalyst surface and the dye, provided by the incorporation of the carbon additive during the synthesis of the semiconductor. The degradation via the chromophore cleavage was also observed (otherwise the reaction would terminate with the formation of the fully N-ethylated intermediate, rendering low photocatalytic yields). RhB photodegradation can also proceed via photosensitization since the pollutant absorbs in the range 460–600 nm; the photosensitized process was not observed in the absence of catalyst

(photolytic breakdown of RhB is low), but it was boosted in the Bi_2WO_6/carbon composites as a result of an efficient injection of electrons from the excited dye to the surface of the catalyst and the strong interactions between RhB and the catalyst surface (Fig. 3) [111]. The acidic sites of the carbon additive seemed strong enough to promote the photosensitized process, in addition to the photocatalytic one. Contrarily, in carbons of basic nature, the interactions between RhB and the surface of the Bi_2WO_6/carbon photocatalysts were weak; hence the degradation occurred only via the photocatalytic process, leading to photooxidation yields very similar to those obtained for bare Bi_2WO_6.

2.3. WO₃/ nanoporous carbon

WO_3 is an n-type semiconductor with electrooptical, electrochromic and catalytic properties [112–114]. WO_3 is considered an interesting visible-light stable photoactive material due to its abundance, low toxicity, physical and chemical resilience in harsh environments, strong absorption features in the solar spectrum (i.e., band gap between 2.4 and 2.8 eV) and high oxidation power of the photogenerated holes due to a deep valence band (allowing the oxidation of water). Nevertheless, pure WO_3 has lower light conversion efficiency than titania, as the reduction potential of the photogenerated electrons in the conduction band of WO_3 is inadequate for direct O_2 reduction [93]. This characteristic provokes the surface accumulation of the photogenerated electrons, causing a high recombination that ultimately reduces the photochemical response [93,115,116]. To compensate for this limitation of WO_3, the use of carbon additives is considered an interesting approach, as the structure of most carbon materials anticipates that the accumulation of electrons may be dissipated by delocalization in the stacked graphene-layers.

Considering all the above, we explored the effect of various carbon additives of varied characteristics in the performance of WO_3/carbon photocatalysts using simulated solar light [105]. We investigated the external quantum yields as a function of the carbon ratio, and correlated the photochemical and photoelectrochemical response of the WO_3/carbon catalysts with the wavelength of the irradiation source, the nature of the carbon additive and the type of photochemical reaction (oxidation of pollutants and water splitting). The photocatalytic runs were carried out allowing the equilibration of the catalysts at dark conditions, which is important when using porous catalysts to counteract
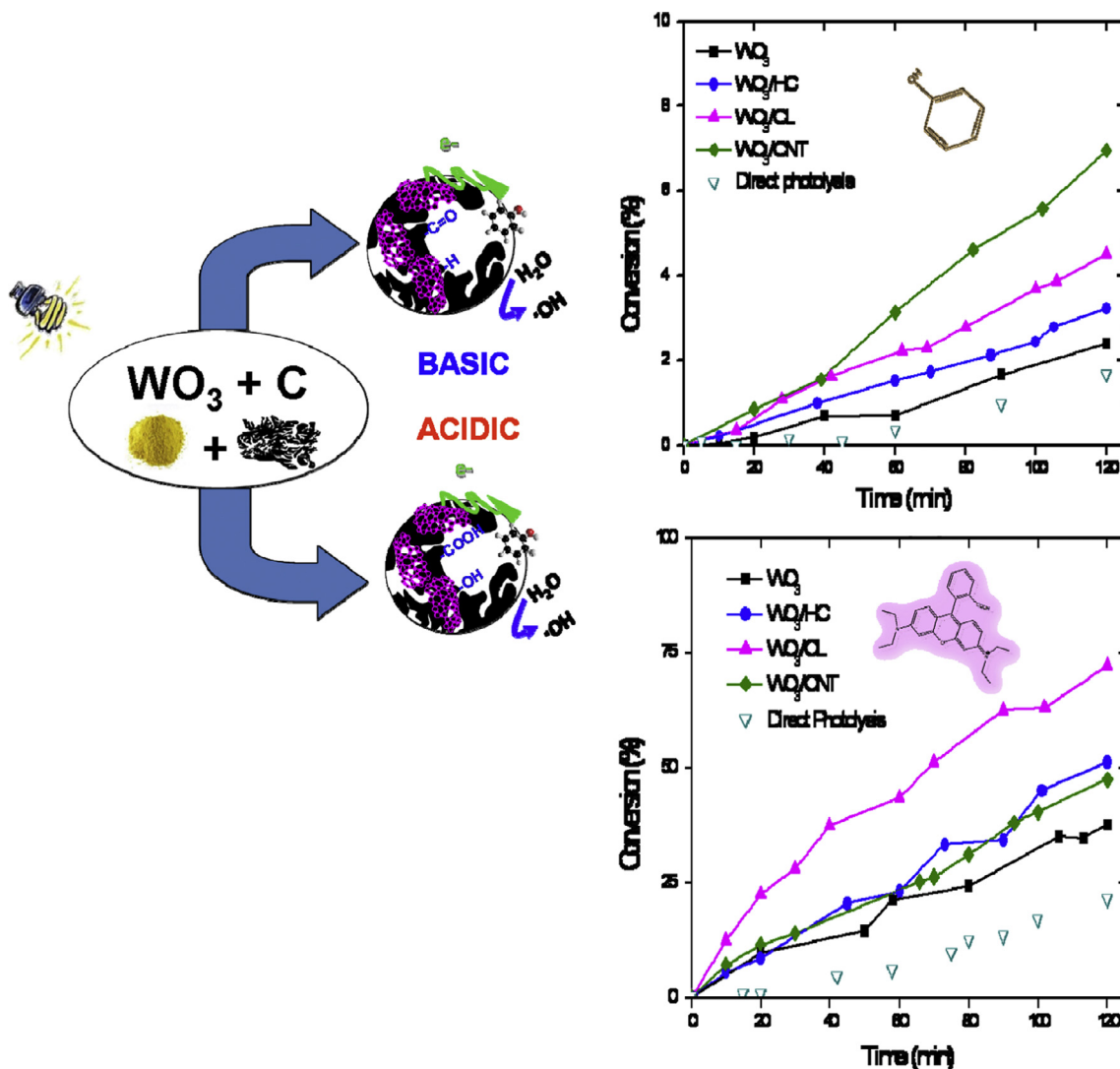
Fig. 4. Schematic representation of the optimized carbon additive for the photodegradation of phenol (top) and rhodamine B (down) under simulated solar lights for various WO₃/carbon photocatalysts (basic carbon nanotubes, CNT, acidic nanoporous carbon, CL, acidic glucose-derived hydrochar, HC).

the adsorption of the pollutant (mainly controlled by the porosity and surface chemistry of the carbon additive). Our results pointed out the importance of the adequate choice of the carbon additive coupled to WO₃, which is also defined by the nature of the pollutant and the interactions at the catalyst-pollutant interface, the latter controlled by the characteristics of the photocatalyst components.

As an example, Fig. 4 shows the evolution of phenol and RhB concentration upon sunlight irradiation of aqueous suspensions of WO₃/carbon mixtures containing ca. 2 wt.% of various carbon additives: commercial carbon nanotubes, an activated carbon and a glucose-derived hydrochar [105]. As seen, the incorporation of the carbon additives improved the photooxidation yields in most cases, but most importantly, different behaviors were obtained for the same carbon additive depending on the target pollutant.

In the case of phenol, an increased photoconversion was observed for all the WO₃/carbon photocatalysts, with higher values for the catalyst containing 2 wt.% of carbon nanotubes. Even though phenol conversion values were quite low for all the WO₃/-carbon mixtures (which is reasonable as phenol is not easily degraded under visible light), the efficiency was higher than that of the photolytic degradation. Interestingly, a clear correlation was observed with the surface acidity/basicity of the carbon. The

photodegradation of phenol was superior in the catalysts incorporating basic carbon additives, indicating that the affinity between the catalyst's surface and phenol molecules is important to obtain high degradation yields. In this regard, it is well known that phenol is preferentially adsorbed on hydrophobic carbons adsorbents via the interaction between the aromatic ring of phenol with the adsorbent's surface [117,118]; hence, a hydrophobic catalyst interface would favor the contact of adsorbed phenol molecules close to the photoactive sites of the catalyst, thereby increasing the photooxidation yield. Additionally, the preferential orientation of the adsorbed phenol molecules in the pores of the carbon favored the regioselective oxidation of phenol in the *ortho* position [49,73].

The same WO₃/carbon catalysts were used for the photocatalytic degradation of a dye (RhB) with strong absorption features in the visible range (Fig. 4). Again, conversions were higher for all the WO₃/carbon photocatalysts than for the unsupported semiconductor. Interestingly, the performance of the materials followed a clear correlation with the acidic nature of the catalysts, as opposed to the trend observed for the degradation of phenol. As discussed above for Bi₂WO₆/carbon composites, this dependence is attributed to the degradation of RhB via coupled mechanisms in acidic photocatalysts (photosensitization, photocatalysis and carbon-photon mediated reactions) [107–109]. Taking into
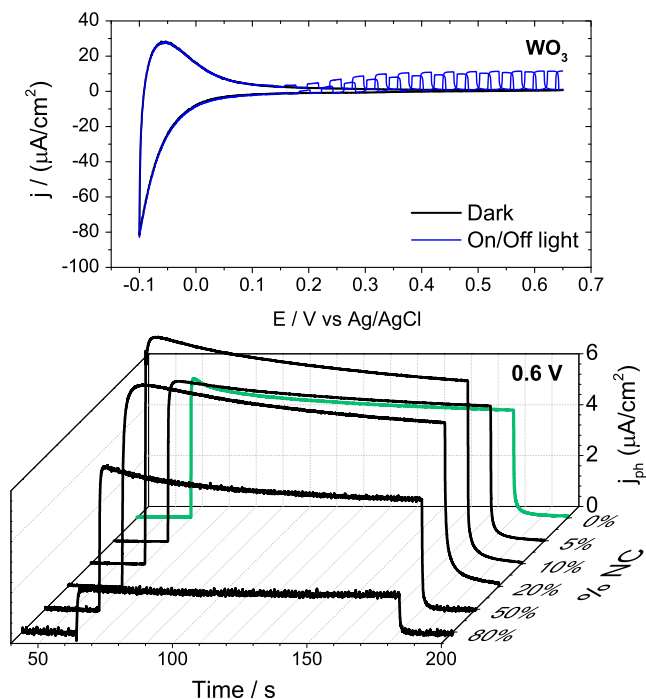
Fig. 5. (top) Cyclic voltammetry of WO$_3$ film recorded at 20 mV/s under dark and square-wave light perturbation with a frequency of 0.5 Hz in 0.5 M Na$_2$SO$_4$ pH 1.3 and (down) transient photocurrent responses of WO$_3$ (0% NC) and hybrid WO$_3$-NC electrodes (percentages of NC ranging form 5 to 80 wt.%) at +0.6 V vs Ag/AgCl under illumination (2 min) using a 371 nm LED. Adapted from Ref. [120].

account the acidity of the WO$_3$/carbon mixtures (in terms of surface pH and hydrophobicity index), the photosensitized mechanism was predominant for all of them.

The superior photoactivity exhibited by the WO$_3$/carbon catalysts for both pollutants has been attributed to different reasons: first, a lower electron–hole recombination rate due to the presence of the carbon component, alleviating the surface accumulation of the electrons via delocalization in the graphenic layers - which in turn extends the lifetime of the charge carriers. This is expected to be the dominant mechanism applying in the case of WO$_3$/CNT, considering the existence of large graphitic domains in the carbon nanotubes that would act as effective electron sinks. The porosity of the catalysts (mainly inherited from the carbon additive) is also important, as well as their acidic/basic nature, as it determines the affinity between the catalysts surface and the target pollutant. For this reason, a hydrophobic environment is desirable for promoting the degradation of phenol molecules, whereas acidic sites are needed to boost RhB degradation [105].

The dissolved molecular oxygen coadsorbed in the pores is also important to promote the participation of the photogenerated electrons in the multi-electron reduction of O$_2$ (O$_2$ + 2H$^+$ + 2e$^-$ → H$_2$O$_2$, and O$_2$ + 4H$^+$ + 2e$^-$ → 2H$_2$O), in a similarly way as reported for metal loaded WO$_3$ [119]. Another possibility is the stabilization of the holes through the oxidation of the water molecules coconfined in the pores of the carbons, leading to the formation of reactive oxygen species (ROS). The ability of the WO$_3$/carbon photocatalysts to form O-radicals was confirmed by spin resonance spectroscopy using a nitrone spin trapping agent [105]. Furthermore, the quantification of the abundance of ROS showed rather constant concentration levels, pointing out that the incorporation of the carbon additive does not affect the ability of the WO$_3$/carbon catalysts to generate species with unpaired electrons.

Besides the photooxidation of organic pollutants, we have also explored the photoelectrochemical response of WO$_3$/carbon elec-

trodes for the oxidation of water. The role of the carbon additive was investigated as a function of the irradiation wavelength, the applied potential bias and the amount of carbon additive over a wide spectral range. For this purpose, WO$_3$/carbon photonodes with increasing amounts of a nanoporous carbon —NC— (ranging from 5 to 80 wt.%) were prepared [120]. Photocurrent transients upon on/off illumination were registered for all studied electrodes at different potentials (Fig. 5). All the transient curves exhibited the characteristic shape of an *n*-type semiconductor, with an initial rapid and sharp photocurrent on switching-on the light, followed by a gradual decay due to trapping of electrons or holes in intermediate surface states and recombination losses [121]. The current retracted instantaneously to its original value when the illumination was switched-off. For carbon contents of 50 wt.% and below, the photocurrent of the anodes were higher than those of the bare semiconductor (normalized photocurrents vs the WO$_3$ content showed a plateau for ca. 20–50 wt.% carbon). This is most remarkable considering that the amount of semiconductor in the anodes is gradually reduced as the amount of carbon additive increases, and demonstrates that these W/NC electrodes are more photoactive than bare WO$_3$.

Incident-to-photon current efficiencies (IPCE) were evaluated for the WO$_3$/carbon electrodes at various wavelengths and bias potentials between 0.2 and 0.6 V vs. Ag/AgCl (Fig. 6). Compared to other materials reported in the literature, these WO$_3$/NC photoanodes rendered relatively low IPCE values [122], indicating that recombination and charge collection are still limiting the efficiency of the electrodes, most likely due to the poor electron conductivity of the nanoporous carbon additive. However, despite the modest IPCE of the WO$_3$/carbon anodes, values were higher than those of WO$_3$ at all applied potentials - with the exception of the electrode with the highest carbon loading-. This is remarkable considering the nature of the carbon additive used in the preparation of the photoanodes (a low cost abundant nanoporous carbon), and offers a new approach that calls out for research in the processing of photoelectrodes using carbons with optimized features (conductivity, surface chemistry and porosity) as sustainable additives. As for the wavelength dependence of the photoelectrochemical response of the WO$_3$/carbon electrodes, higher photocurrents were obtained between 360 and 500 nm (photocurrent densities ca. 3–4 times higher than for bare WO$_3$). This confirmed that the effect of the carbon additive affects both the UV and the visible range (Fig. 6).

Overall, the superior performance of the photoanodes after the incorporation of increasing amounts of the nanoporous carbon additive was attributed to the improved electron collection provided by the carbon component, which facilitates the electron transfer to water molecules at the photocatalyst/electrolyte interface. Additionally, in nanoporous electrodes the diffusion length of the minority carriers is small due to the nanometric dimensions of the pore voids, reducing the probability of recombination. Although similar responses had been reported using carbon nanotubes and graphene-derived carbons, we herein demonstrated that this behavior can also be achieved with low-cost nanoporous carbons with a disordered turbostratic structure.

3. Photochemical behavior of nanoporous carbons

3.1. Photooxidation of pollutants

Despite the interesting optical features reported for graphene, carbon nanotubes and other forms of carbons, there has been a dearth in exploring the photocatalytic activity of carbon materials themselves. In 2009, Luo et al. reported the first evidence on the photoactivity of carbon nanotubes under visible light, attributed to the presence of structural defects and vacancies [123]. Later, a
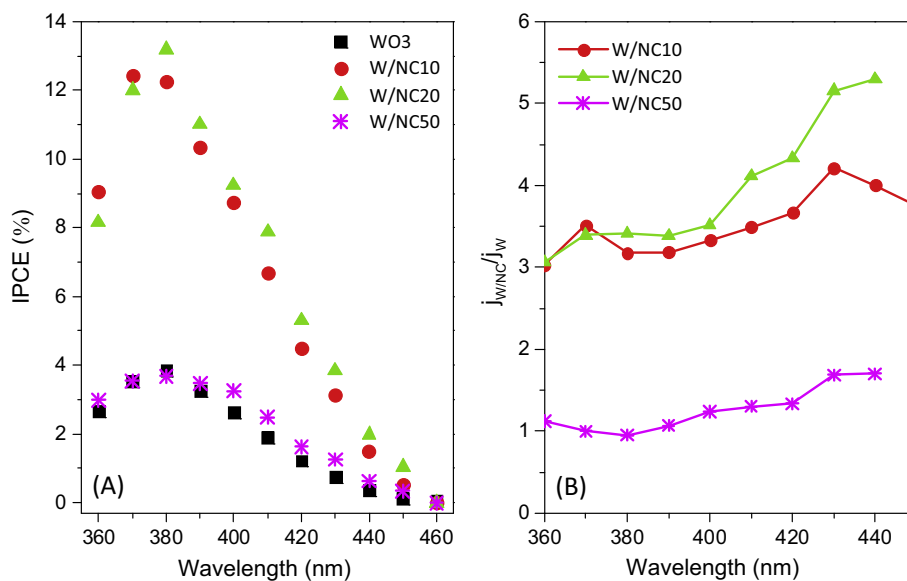
Fig. 6. Dependence of the (A) IPCE values and (B) normalized photocurrent densities (jW/NC$_x$/jWO$_3$) on the wavelength of the illumination source (bias potential of +0.6 V vs Ag/AgCl, irradiation with a Xe lamp fitted to a single-pass monochromator) for WO$_3$ and WO$_3$/carbon anodes (W/NC$_x$, x = wt.% of the carbon additive NC). Reprinted from Ref. [120].
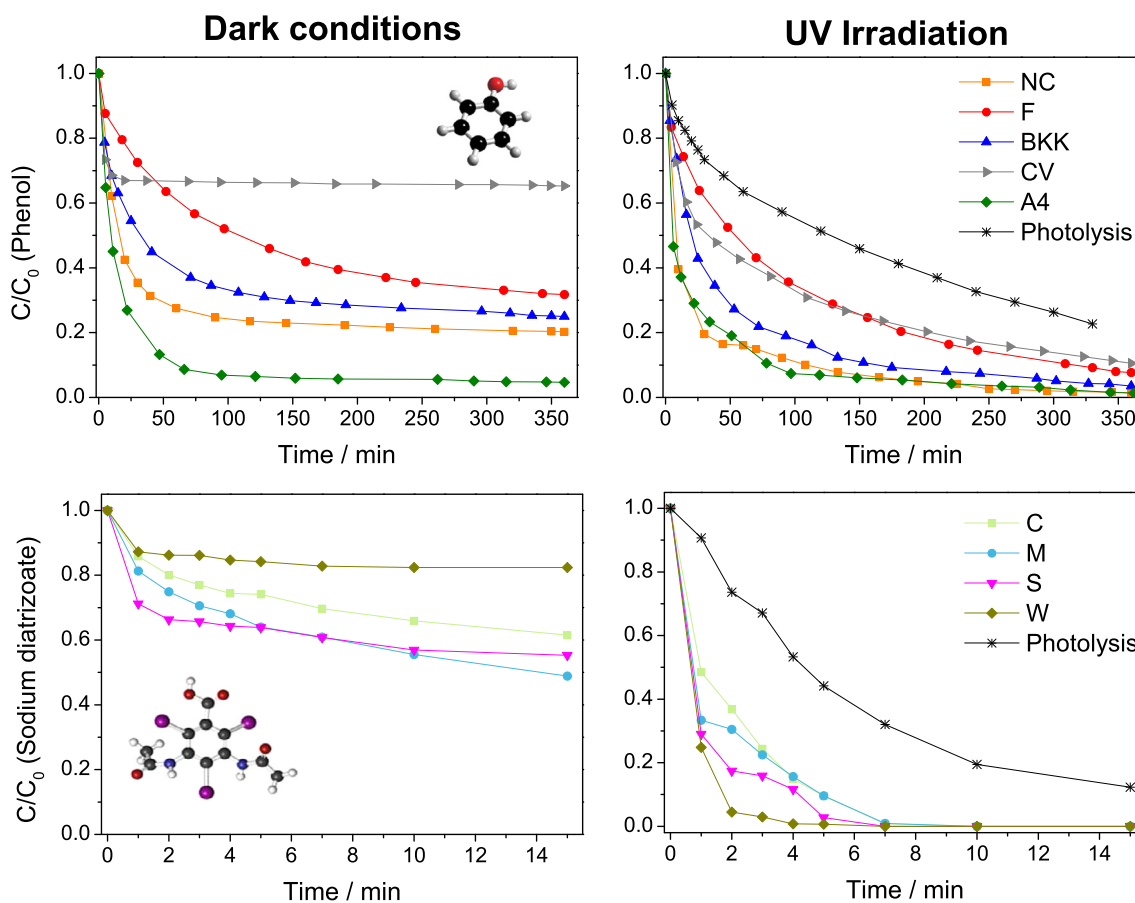
Fig. 7. Concentration decay curves of phenol (A, B) and DTZ (C,D) on various nanoporous carbon photocatalysts under dark (A,C) and UV irradiation (B, D). Panels A, B are reprinted from Ref. [43], copyright 2012, with permission from Elsevier.

few works reported the activity of graphene-based nanocomposites [124,125]. However, knowledge on nanoporous carbon/semiconductor photocatalysis has traditionally been associated to the role of carbons as non-photoactive supports [30,67], and the

enhanced performance of the carbon/semiconductor composites had been almost exclusively discussed in terms of the texture and/or the electronic conductivity of the carbon (see above discussion).

In 2010 we showed that a nanoporous carbon used as support in carbon/TiO$_2$ composites was capable of a significant level of self-photocatalytic activity under UV–visible irradiation, outperforming bare or immobilized titania [42,43]. The work provided the proof of the concept for the photocatalytic activity of nanoporous carbons in the absence of semiconductors. Aiming at understanding this behavior and the mechanisms governing the photochemical activity of carbons, we continued this research line and explored the photooxidation of pollutants in water (e.g., sodium diatrizoate, phenol, rhodamine B) using nanoporous carbons as photocatalysts, settling the basis for a future implementation in carbon-based advanced oxidation processes for water treatment [42,43,126].

Experiments were carried out by irradiation of suspensions of the nanoporous carbons in contact with aqueous solutions of the target pollutants. During these photocatalytic assays, several processes may occur simultaneously-degradation due to photocatalyzed and/or photolytic (non-catalyzed) reactions, and removal due to adsorption in the porosity of the carbon material-, for which evaluation of the quantum efficiency or turnover of nanoporous catalysts becomes a complex issue, and thus different approaches must be envisaged.

For instance, Fig. 7 shows the rate of phenol disappearance upon UV–vis irradiation of several nanoporous carbons); the increased overall removal rate under irradiation compared to dark conditions (where removal is due to adsorption) corroborated the photoactivity for the series of carbons in absence of semiconductor [43]. The trend was more remarkable for carbons of acidic nature, where phenol removal increased from 35% in the dark to 90% under irradiation. The relative abundance of the degradation intermediates detected in solution also showed a dependence on the characteristics of the carbons, with a marked regioselectivity for the formation of catechol over quinones (as opposed to the phootoxidation using titania). Similar observations have also been reported for carbon/TiO$_2$ photocatalysts [30,76]. It should also be pointed out that some nanoporous carbons exhibited similar performance in dark and under illumination [43], suggesting that the photocatalytic activity does not apply for all type of nanoporous carbons,

but it should be somehow related to their physicochemical and/or structural features. This would explain why most studies in the literature had reported the non-photoactive behavior of activated carbons [30,127].

The photocatalytic activity of nanoporous carbons was also studied for the photooxidation of some other pollutants. For instance, Velo-Gala et al. analyzed the behavior of commercial nanoporous carbons under UV light [126] for the photooxidation of sodium diatrizoate (DTZ), a recalcitrant emerging pollutant widely used in hospitals as iodinated contrast and detected in urban wastewaters, surface waters, and ground waters [128–132]. The carbons were used as received and after chemical modification, so as to obtain a series of carbons with similar textural characteristics but different surface chemistry [133]. For all the studied carbons, the DTZ removal rate due to the photodegradation process (excluding direct photolysis and adsorption removal) was enhanced in the presence of the carbons, ranging from 14 to 90%, depending on the activated carbon (Fig. 7).

To determine if nanoporous carbons as photocatalysts fulfill the requirements of long cycle-life and good degradation efficiency, we studied the performance of several nanoporous carbons with different surface chemistry towards the photodegradation of phenol and sodium diatrizoate during consecutive runs [47,126]. Fig. 8 shows the evolution of phenol photooxidation with the nanoporous carbons upon six consecutive cycles, where it can be observed that the performance of the carbons was comparable to that of TiO$_2$. The photocatalytic efficiency was found to depend strongly on the basic/acidic nature of the nanoporous carbons, with a somewhat lower performance for the hydrophilic catalysts. A marked accumulation of aromatic degradation intermediates in the solution was observed during the photocatalytic cycles using the nanoporous carbons, with preferential formation of catechol over quinones. For titanium oxide, the amount of aromatic intermediates detected in solution was lower, but the accumulation of short alkyl chain organic acids was also observed, leading in both cases to poor mineralization values upon cycling. Conversion yields and mineralization rates were greatly enhanced in the presence of excess of dissolved oxygen in the solution regardless the nature
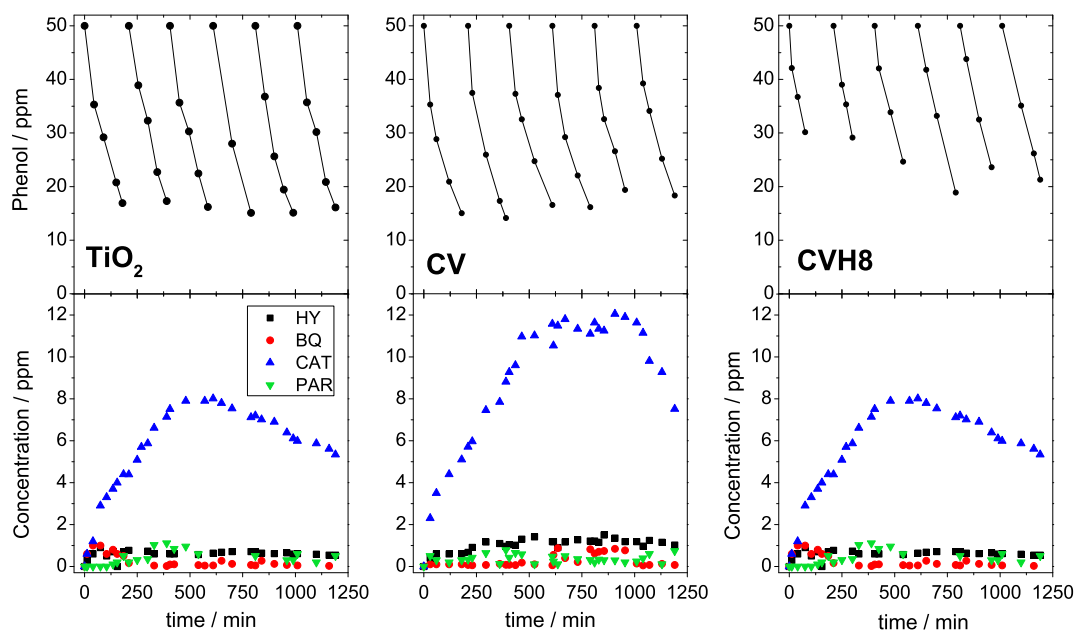
Fig. 8. Evolution of phenol concentration (top) and its main degradation intermediates (bottom) after several consecutive photocatalytic cycles on nanoporous carbon CV and CVH, and TiO$_2$ (P25, Evonik) under excess oxygen supply. Hydroquinone (circles); benzoquinone (down triangles); catechol (squares); 2,4,6-trihydroxybenzene (up triangles); resorcinol (crosses); 1,3,5-trihydroxybenzene (diamonds). Adapted from Ref. [47], copyright 2014, with permission from Elsevier.

of the pollutant to be degraded. This was critical for the long-term performance of the hydrophilic carbon (which showed a sharp fall in conversion upon cycling under oxygen depletion conditions), and pointed out to the formation of radical species upon illumination of the nanoporous carbons.

To understand the origin of the photochemical response of semiconductor-free nanoporous carbons, several possible scenarios were considered [43]: (1) the adsorption/desorption of the pollutant and photooxidation intermediates on the porosity of the carbon materials, causing an enhancement in the conversion due to the effect of the pollutant concentration on the photocatalytic reaction; (2) the occurrence of carbon/light interactions that would provoke the degradation of the adsorbed compounds retained in the pores of the carbon; (3) the formation of radical species upon illumination of the carbons. The unbalance between the amount of compounds detected in solution and that retained in the porosity after the photocatalytic runs demonstrated that the differences in conversion (rate and intermediates speciation) under dark and irradiation conditions cannot be explained by the confinement of the pollutant in the porosity (scenario 1) [43]. The occurrence of the existence of carbon/light interactions that would provoke either the degradation of the pollutant inside the porosity of the carbons (scenario 2), and/or the formation of O-radical species in aqueous environments (scenario 3) was explored by combining spectroscopic and photoelectrochemical tools [43].

3.1.1. Optical band gap of nanoporous carbons

Insights on the mechanisms occurring at the nanoporous carbon/water interface when exposed to light were obtained investigating the optoelectronic and photoelectrochemical response of the nanoporous carbons. The optical band gap energy of the carbons was explored using diffuse reflectance spectroscopy over the range 200–2000 nm (ca. 6.20–0.62 eV); samples were prepared by mixing the nanoporous carbons with barium sulfate (ratio 1:10) [126]. For different transition mechanisms, it has been demonstrated that the energy of the optical band gap (Eg) depends on the absorption coefficient of the material (α) and the photon energy (hν), following the equation: $\alpha \times h\nu = C(h\nu - Eg)^n$, where n is a constant that determines the type of optical transition (direct/indirect allowed/forbidden transitions). Since the Kubelka–Munk theory [134] correlates the absorption coefficient of a material with the diffuse reflectance through the F(R) function, Eg can be determined by plotting $[F(R) h\nu]^{1/n}$ vs hν [135,136]. The determination of Eg is controversial because of the incertitude concerning the value assigned to n, and the method for calculating the band gap. In our case, the value of Eg was obtained considering n = 1/2 for allowed direct transitions, as suggested by various authors [137–139]. Additionally, a double liner fit [140] was used

to minimize the error associated to the graphical determination of Eg value; an example is depicted in Fig. 9A.

Values lower than 4 eV were reported for several nanoporous carbons, which are in agreement with the photoactivity detected under UV light for all of them. Indeed, photodegradation rate constants were nicely correlated to the band gap values of the carbons, with the highest rates obtained for the nanoporous carbons with lowest Eg values [126]. Additionally, surface functionalization of the carbons was found to have a strong effect on the optical band gap of the carbons; those materials with high surface oxygen, presented lower Eg values (Fig. 9B), whereas the photocatalytic activity was found to correlate with the density of ester/anhydride groups decorating the carbon surface, as well as the sp^2/sp^3 ratio.

3.1.2. Detection of O-radical species upon irradiation of nanoporous carbons

The dependence of the photochemical activity of the nanoporous carbons on the presence of dissolved oxygen suggested the formation of O-radical species upon irradiation of the carbons. Although the ability to photogenerate radicals is well-established for inorganic semiconductors or carbon/semiconductor composites [141], this issue was not so clear for nanoporous carbons. To address this question, we investigated the formation of paramagnetic species using electron spin resonance spectroscopy (ESR) and chemical trapping agents (e.g., DMPO, DEPMPO) that are capable of forming spin adducts with specific radicals, easily detected by various techniques [44,48,49,142].

Fig. 10 shows the ESR spectra corresponding to the DMPO-adducts obtained upon irradiation of carbon suspensions in water, as well as those corresponding to TiO$_2$ as benchmark semiconductor. All the samples (carbons and titania) showed a quartet peak profile with 1:2:2:1 pattern of intensities, characteristic of DMPO-OH adducts [143], although some other adducts with a different pattern, identified as HDMPO-OH, DMPO-R (carbon centered radical) and DMPO-OOH, were also identified.

The detection of the DMPO-adducts confirmed the formation of hydroxyl and/or superoxide radicals during the irradiation of the carbons in aqueous medium; this demonstrated the formation photogenerated charge carriers (electrons and holes) upon irradiation of the carbons, and their stabilization through reactions with dissolved oxygen and water adsorbed in the nanopores of the carbons. The stabilization of the holes through the oxidation of water would form hydroxyl radicals, while the electrons participate in the multi-electron reduction of molecular oxygen to produce superoxide radicals and hydrogen peroxide, which may be further reduced to hydroxyl radical (HO$\cdot$) or water, according to the reactions:
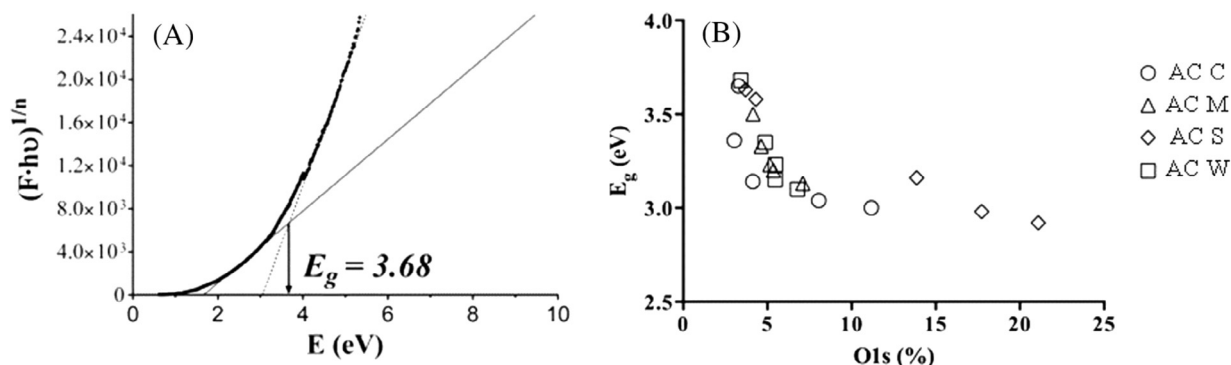
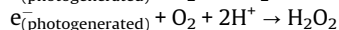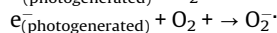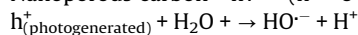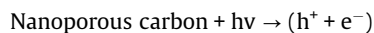**Fig. 9.** (A) Example of the mathematical approach to evaluate the optical band gap energy (Eg) of nanoporous carbons; (B) correlation between the Eg value and the amount of surface oxygen on various nanoporous carbons. Adapted from Ref. [126], copyright 2013, with permission from Elsevier.
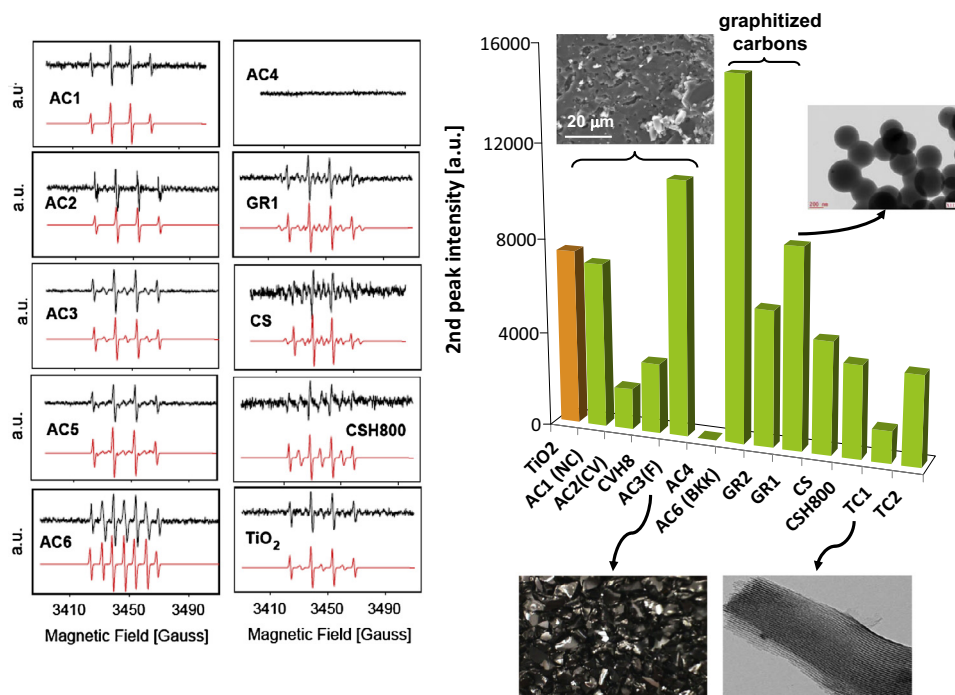
Fig. 10. (left) Experimental (top, black) and simulated (down, red) ESR spectra of selected nanoporous carbons and commercial titania powders (P25, Evonik). Reprinted from Ref. [44], copyright 2013, with permission from Elsevier. (right) Quantification of the radical species detected from the ESR signals corresponding to DMPO–OH adducts (second peak intensity in the 1:2:2:1 patterns) for the nanoporous carbons (selected TEM and SEM images of the carbons are also shown for clarity).

Nanoporous carbon + hv → (h$^+$ + e$^-$)

h$^+_{(photogenerated)}$ + H$_2$O + → HO$^{\cdot-}$ + H$^+$

e$^-_{(photogenerated)}$ + O$_2$ + → O$_2^{\cdot}$

e$^-_{(photogenerated)}$ + O$_2$ + 2H$^+$ → H$_2$O$_2$

Quantification of the abundance of the radical species showed higher DMPO-OH concentration levels for certain carbons than for titania [44,45,142]. As for the nature of the carbon material, as a general rule, lower ESR signals were obtained for carbons with

a rich surface chemistry. On the other hand, for some carbons no radicals were detected by ESR, which seemed to be in agreement with the lack of photoactivity observed for this material in previous works [43], and demonstrated that formation of photoinduced radicals is not an intrinsic property of all carbon materials.

It should also be pointed out that some carbons with a rich chemistry and showing low concentration of radical species displayed among the highest photocatalytic activity towards phenol
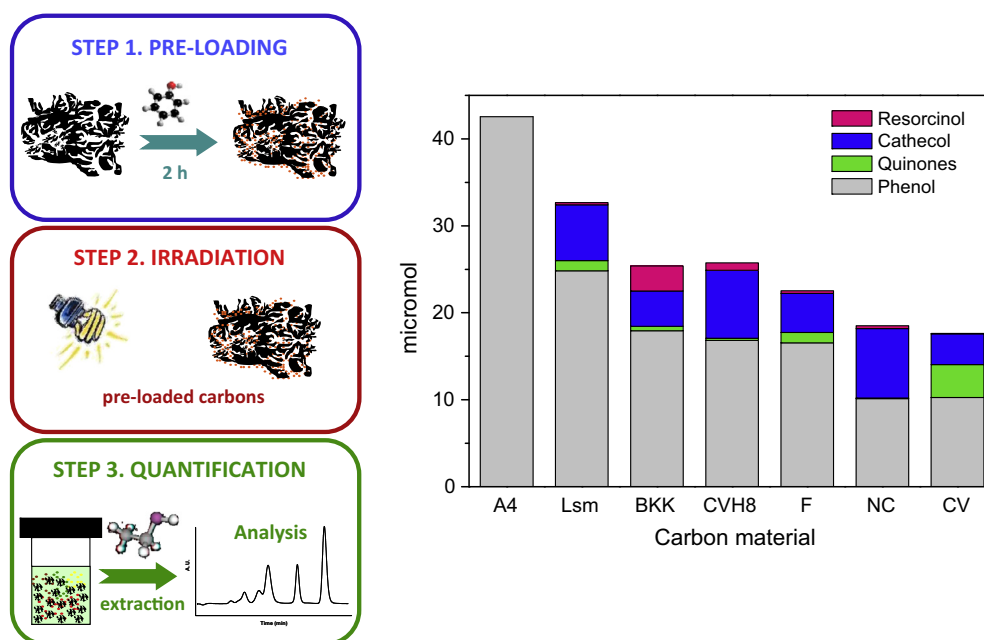
Fig. 11. (left) Schematic representation of the experimental approached designed for evaluating the photocatalytic activity inside the nanoporosity of carbon materials. (right) Quantification of the species detected in the extracts of a series of preloaded nanoporous carbons after UV irradiation for 20 min.

photooxidation [43–45], higher than other carbons with larger ESR signals. A similar finding was obtained for some titanium oxides powders, where the lack of ESR signal was accompanied by a non-negligible photocatalytic yield, and this has been attributed to a direct hole transfer mechanism rather than a radical-mediated one [144]. Thus, even though ESR spectroscopy may contribute to the understanding of the photochemical response of carbon materials, it just provides a diagnostic indication of formation of free radicals. Hence low ESR signals should not be considered as an indication of low photoactivity, but rather to the predominance of a radical-mediated or direct hole transfer degradation mechanisms.

More recently, we have also demonstrated the formation of hydroxyl and superoxide radicals upon irradiation of nanoporous carbons using solar light, quantifying the concentrations of both radical species using chemical trapping agents for various carbon loadings and reaction times [145]. Concentrations of superoxide anion and hydroxyl radicals were found to depend on the surface chemistry of the activated carbons, with carbons with low band gap values favoring the formation of the latter.

3.1.3. Photocatalysis in the confined porosity of nanoporous carbons

As mentioned above, when using porous catalysts, the photocatalytic degradation becomes a complex process since several phenomena can coexist (adsorption, desorption and diffusion of different species in solution, photolytic breakdown in solution, photocatalyzed reactions inside the pores). To discriminate the contribution of the carbon/light interactions from the other secondary reactions, we developed a new approach based on monitoring the photodegradation reaction from a different viewpoint and consisting on carrying out the irradiation of the carbons preloaded with the target pollutant and analyzing the evolution of the species both in the aqueous phase and inside the porosity of the carbon (Fig. 11). This approach allows neglecting the effects of adsorption kinetics and solution photolysis [47–49,142].

Fig. 11 shows the data obtained for the photooxidation of phenol in various preloaded carbons, determined by solvent extraction (no lixiviation towards the solution was detected for any of the carbons). The conversion of phenol inside the carbons was larger or similar than in the photolytic reaction, with differences in the distribution and nature of the intermediates. This is most outstanding considering that the incident photon flux arriving at the phenol molecules adsorbed in the porosity of the carbons is much smaller
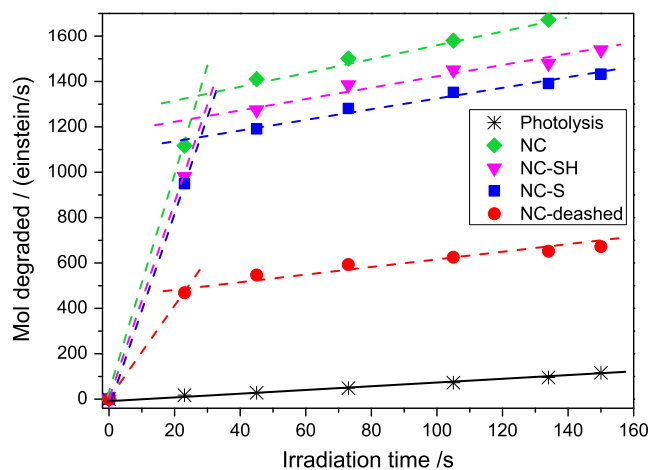
than that from solution (due to the strong shielding effect of the carbon matrix) [43,142]. For one of the studied carbons the extent of photodegradation inside the porosity was negligible, indicating that the photochemical response of the carbons does not only depend on the confinement of the pollutant, but it must also be related to the nature of the carbon, likely composition, surface acidity/basicity, structure, etc. [43].

In an attempt to quantify the efficiency of phenol degradation in the confinement of the porous network of the carbons, we estimated an apparent or pseudo photochemical quantum yield (Φps) [43,49]. Due to the fraction of light absorbed by the carbon matrix, and the light scattering by the catalyst particles suspended in solution, the evaluation of the accurate incident photon flux (needed for the evaluation of the quantum yield) is very complex. Thus Φps was estimated considering that all photons are absorbed by the solution (the actual incident photon flux that reaches the phenol molecules preadsorbed in the carbon matrix is certainly much lower than that in the photolytic reaction and that provided by the lamp, where neither light scattering nor catalyst absorption occur). This approximation cannot be considered *stricto sensu* a quantum yield, but would account for the minimum limit of the actual quantum yield, allowing the comparison of the different nanoporous carbons. The pseudo-quantum yield obtained for the different studied carbons is shown in Fig. 12. In solution (photolysis) the plot of the number of mol of degraded phenol per incident photon flux vs the irradiation time is a straight line, yielding Φ = 11 mmol/Einstein, which is in good agreement with other values reported in the literature [146–148]. More importantly, Φ_{PS} values estimated for the nanoporous carbons were higher than the one retrieved from solution. The evolution of Φ_{PS} over time showed two different regimes: below 30 min of irradiation an extremely high degradation yield is observed (Φ_{PS} close to unity), followed by a second linear region where Φ_{PS} is still 5 times higher than the value obtained for the solution photolysis. These two regimes could be related to the consumption of coentrapped water and/or oxygen in the first stage, leading to a diffusion limited rate in the second one [43,49].

To further comprehend the effect of nanoconfinement and its dependence on the characteristics of the nanoporous carbons and on the wavelength of the irradiation source, we investigated the photochemical activity using monochromatic light on a series of nanoporous carbons obtained from different precursors [47], and exhibiting controlled porous features [142] and surface chemistry [45,48], choosing phenol phootoxidation as model compound.

Fig. 13 shows the wavelength dependence of the photodegradation of phenol inside the porosity of various carbon materials from

Fig. 12. Pseudo photochemical quantum yield (Φps) of a series of nanoporous carbons: NC, pristine carbon; NC-S, carbon NC oxidized in ammonium persulfate; NC-SH, sample NC-S treated at 400 °C under inert atmosphere; NC-deashed, NC carbon after removal of ashes by acid digestion in HF/HCl.
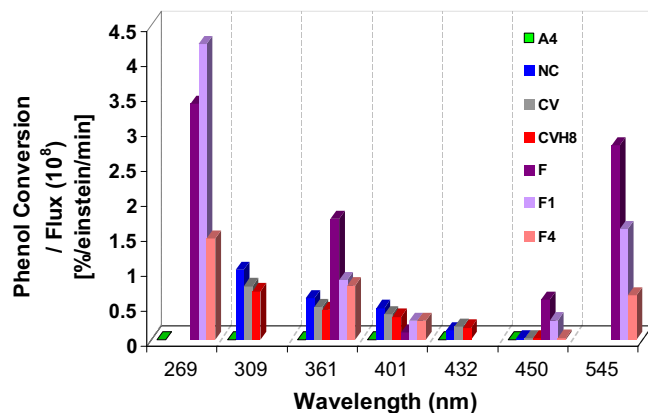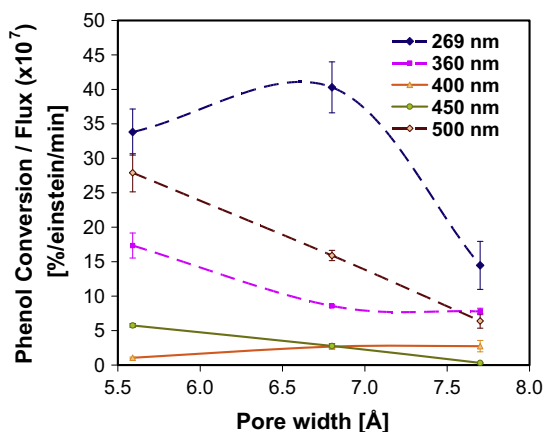

Fig. 13. Phenol conversion normalized per incident photon flux under monochromatic light on a series of nanoporous carbons.
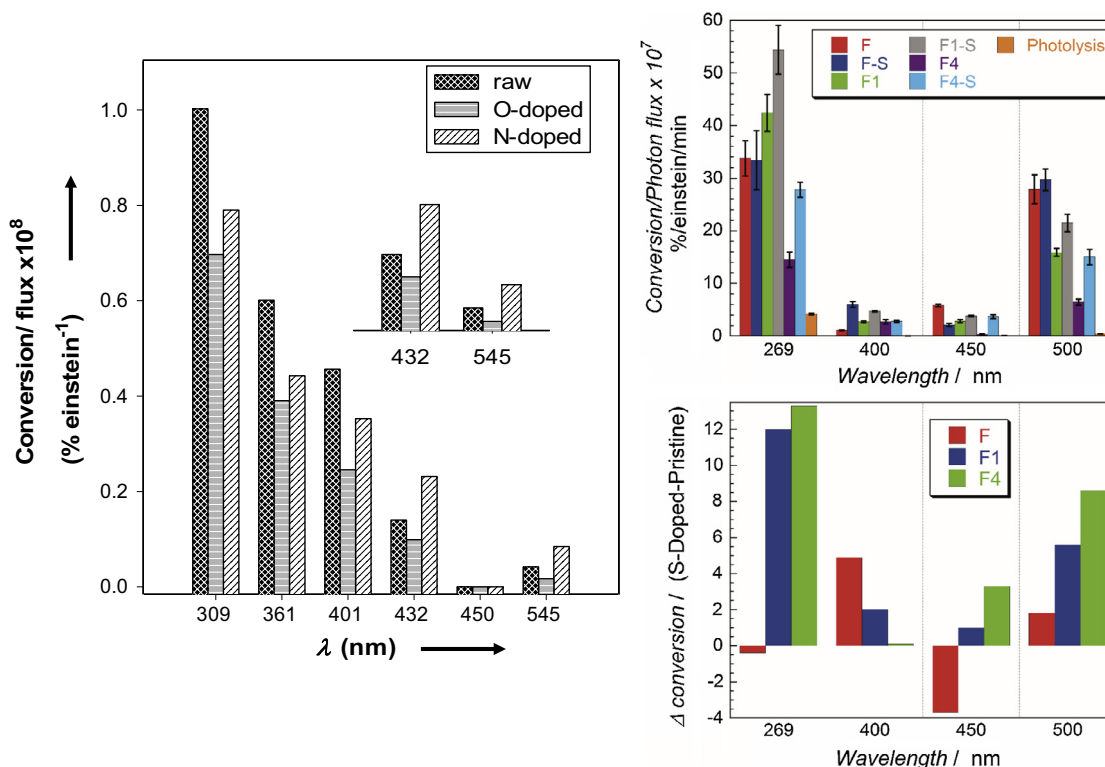
Fig. 14. Dependence of the normalized phenol photooxidation conversion on the average micropore size evaluated from gas adsorption data. Reprinted from Ref. [142].

432 nm for the carbon materials, which corresponds to over 100 nm redshift compared to the non catalyzed reaction.

The correlation of the yield of the photochemical reaction at various wavelengths to the carbon's average nanopore size also revealed interesting features (Fig. 14) [142]. A U-shaped pattern with the wavelength was observed again, with the minimum featuring at about 400 nm. As a general trend, the photochemical conversion of phenol gradually decreased with the enlargement of the average micropore size, being the effect less remarkable at high wavelengths. Data also showed that there is a threshold pore size for an optimum exploitation of the light, which is connected with the dimensions of the target molecule retained in the porosity and the strength of the interactions between the pollutant and the nanopore walls. At 269 nm the light conversion for phenol oxidation was enhanced for pores below 0.7 nm, whereas the photochemical response was drastically reduced when the pores were widened by 0.1 nm. Similar patterns were obtained for higher wavelengths, although the drop in the conversion was pronounced. This trend is attributed to the tight confinement of phenol molecules in the narrow microporosity of the carbon, maximizing host-guest interactions [117,118]. When the pore aperture was enlarged, the interactions between the adsorbed phenol molecules and the pore walls became weaker [149], thus decreasing the probability of the fast charge transfer of the photogenerated carriers. In this situation, other electron donors and/or holes scavengers present in the medium (i.e., oxygen, water molecules) compete with adsorbed phenol molecules, resulting in lower conversions.

To establish a relationship between the chemical functionalization of nanoporous carbons with their photochemical response, several carbons were chemically modified to introduce O-, N- and S-containing groups [46,48,49]. As seen in Fig. 15, the functionalization with N- and O-groups brought about small changes

different origins using monochromatic light. With the exception of one carbon, all the samples showed photochemical activity in the visible range (ca. above 432 nm). The performance followed a U-shaped pattern with the wavelength, with a minimum of conversion between 400 and 450 nm. This trend was obtained for various carbon materials and using different lamp set-ups [46], thus allowing to discard any effects from the incident photon flux. Nevertheless, the most outstanding conclusions inferred from this study were the demonstration of the photochemical activity of nanoporous carbons under visible light, and the fact that the onset of phenol photooxidation reaction shifted to wavelengths as high as

Fig. 15. (A) Effect of surface functionalization on phenol conversion values per incident flux upon illumination at different wavelengths using monochromatic light provided by a Hg lamp. Reprinted with permission from Ref. [46]. Copyright 2014, Wiley. (B) (top) Normalized phenol conversion per incident photon flux at different wavelengths for a series of S-functionalized nanoporous carbons with different average pore size and (bottom) effect of sulfur on the conversion of phenol, defined as the difference between the conversion in the S-functionalized and its corresponding as-received carbon. Reprinted from Ref. [142].

in the overall photooxidation yields, with phenol conversions following the trend: pristine $\sim$ N-doped > O-doped carbon. As the chemical modifications did not modify the textural parameters of the carbons, this behavior was exclusively associated to the differences in surface chemistry. Interestingly, the oxidation of the nanoporous carbons decreased the photochemical conversion of phenol in the confined nanopore space [49], which contrasts with other studies from the literature reporting an increased performance towards the oxidation of other pollutants after the incorporation of O-groups in the carbon matrix [41]. This apparently contradiction is explained by the impact of the oxidation treatment on the interactions between the carbon material and the target pollutant, which govern the conversion inside the porosity (ca. oxidation of the carbon results in lower phenol affinity).

The most interesting finding of this study was the wavelength dependence of the photochemical response after the chemical modification [46,142]. Whereas the oxidized carbons showed a similar trend than the pristine material, N-functionalization (mainly in the form of quaternary nitrogen and pyridine-type groups) provoked a redshift in the light absorption features (seen in the increased conversion at 432 and 545 nm). These differences are explained in terms of the changes in the π electron density of the graphene sheets of the carbon matrix upon functionalization. For O-groups, the fall in phenol photooxidative conversion can be attributed to the electron withdrawal effect of the functionalization on the carbon, which would affect the stabilization of the photogenerated carriers by delocalization within the carbon basal planes. On the contrary, nitrogen moieties are known to increase the polarity and the electron transfer properties of carbon due to electron-donating character of the lone pair of electrons of the nitrogen atoms [150] and favoring interlayer bonding. Furthermore, N-functionalization is expected to modify the density of electronic states of the carbon material, likely by introducing intermediate states of higher energy between the conduction and valence band [151,152]. Such intermediates states would act as stepping stones facilitating the absorption of low energy photons, accounting for the photochemical activity at wavelengths corresponding to the visible light, as opposed to the pristine carbon.

For the incorporation of S-groups (Fig. 15), the general trend showed an improved photoactivity with the sulfur content at all the wavelengths, particularly at 269 and 500 nm, demonstrating the enhanced exploitation of light in the UV and visible ranges [48,126]. A positive effect of S-functionalization has been also reported for the photoelectrochemical splitting of water using nanoporous carbons and polychromatic light [50]. The photochemical response of the carbons was strongly influenced by the chemical environment of the S-groups, with oxidized forms of sulfur being more photoactive than thiols and/or sulfides. Several scenarios have been discussed to account for the improved photochemical activity of the S-functionalized carbons. First, the incorporation of sulfur provoked a narrowing of the average pore size, thereby boosting the separation of the photogenerated charge carriers by increasing the probability of the reaction with the adsorbed phenol molecules (trapped in the pores) [49]. The fast charge transfer is favored in S-functionalized carbons, as the presence of heteroatoms is known to lower the energy difference between the electronic levels of the carbons [150,153]. Second, the stabilization of the holes through the oxidation of water coadsorbed in the pores is also expected. This was corroborated by ESR using a nitrone as trapping chemical. Additionally, based on the role of the N-, S- and O-containing groups, we proposed some other transitions involving the activation of chromophoric groups on the carbon surface under visible light [47,49,50].

Summarizing, the light absorption features of amorphous carbons have been reported to depend on the Density Of electronic States, DOS, which energy spread of states depends upon the sp^2/

sp^3 hybridization ratio of the carbon atoms, and the electronic transitions involving the sp^2 carbon clusters [154–156] and/or the activation of chromophoric groups on the carbon surface [50,157]. The size and ordering of the sp^2 clusters, their population in the carbon matrix and the creation of distortions of π^* states have been suggested to have a strong effect in the optical characteristics of the carbons. Upon irradiation of the carbons, excitons (holes or electrons) are formed and if their recombination is delayed they can participate in charge transfer reactions with electron donors (Fig. 16). Regarding the nature of the excitons, in the UV range, medium to low range ones Frenkel-like created in the π-π^* and σ-π electronic transitions involving zig-zag, carbine-like sites and other intermediate states [151,154,155] are expected to be dominant in carbons nanoporous of low functionalization (with dielectric constants lower than those of n-type semiconductors and higher than those carbon blacks, graphene or fullerenes) [158,159]. In functionalized carbons, charge-transfer excitons formed by localized states involving O-, S- and C-atoms may also be formed. Additionally, N-, S- and O-containing groups can act as chromophores, photogenerating excitons that also participate in the observed photochemical reactions [160,161]. The photogenerated electrons are delocalized through the sp^2 carbon domains, allowing the participation of the holes and electrons in some other electronic transitions with acceptors present in the medium. (i.e., water, oxygen, surface groups, pollutants). Furthermore, the electron transfer is facilitated in functionalized carbons, as the energy difference between the electronic levels is lower than that in pure carbon units [150].

3.2. Photooxidation of water

The catalytic water splitting to produce hydrogen and oxygen is a key process for solar fuel production systems towards a sustainable utilization of electricity generated from renewable energy resources. From the large scale application point of view, water breakdown by electro- and/or photoassisted methods has been hampered by the low overall efficiency of the reaction - mainly due to the sluggish kinetics of oxygen evolution and the large overpotentials needed- and the scarcity and high cost of the precious metals used as catalysts (RuO_2 and IrO_2, and Pt/C are currently the most efficient catalysts towards the oxygen evolution and reduction reactions, OER and ORR, respectively) [162–167]. Research on the use of more abundant materials that can server as efficient catalysts in such systems has received much attention [168–173]. Although it has been known for some time and intensively investigated, that graphene (either itself or coupled with other active materials) is able to catalyze the water splitting reaction (mainly ORR) in alkaline media, research on the use of nanoporous carbons for this reaction has not received much attention [50,157].

Following our results on the photochemical activity of nanoporous carbons towards the oxidation of pollutants and their ability to generate radical species in water, we decided to explore their use as photoanodes in the photoelectrochemical water-splitting [49,50,174]. Compared to other studies on metal-free carbon photoanodes [175–178], we used low cost nanoporous carbon anodes obtained from an organic polymer precursor – i.e., poly(4-ammonium styrene-sulfonic acid) and coal (physical activation). The materials were selected based on their textural features and rich surface chemistry (via O-, S- and N-functionalization) that was also tuned by wet oxidation in mild conditions so as to control the density and nature of the O-moieties decorating the edges of the graphene layers, the specific textural and structural features and the self-photochemical activity recorded in solution.

For the carbons synthesized from the organic polymer precursor (samples CONS and CONS-I in Fig. 17), a remarkable photocur-
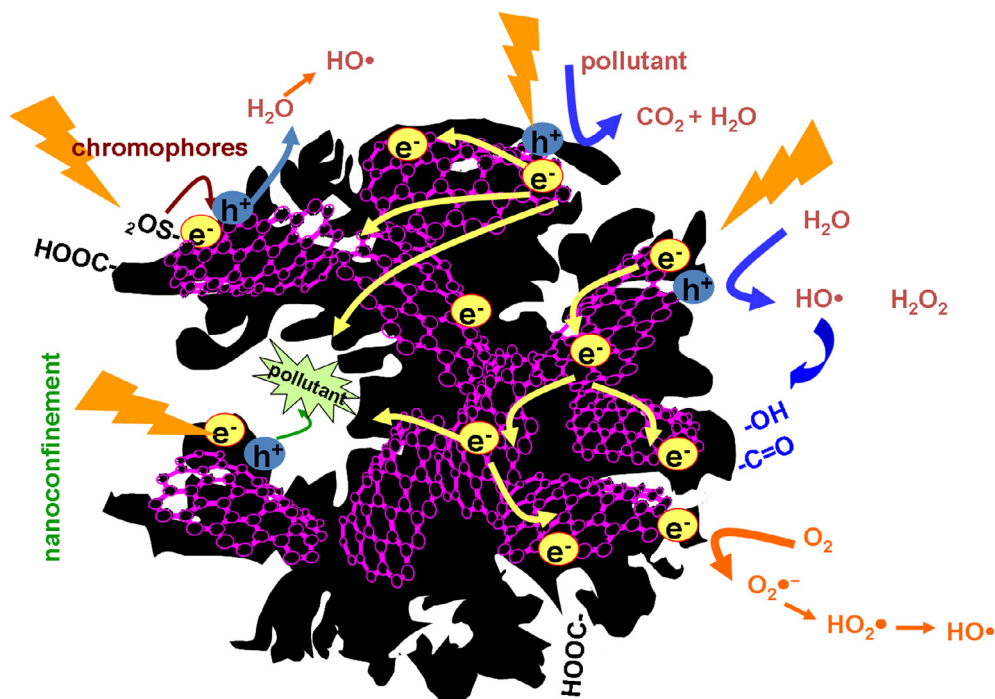
Fig. 16. Schematic representation of the mechanism proposed for the exciton formation and fate upon irradiation of nanoporous carbons.

rent was generated at an overpotential of 0.8 V vs Ag/AgCl, clearly lower than the value recorded for the naked current collector [50]. In an aqueous electrolyte in which water molecules are the only hole scavengers, the anodic photocurrent corresponds to water oxidation (this was also corroborated by measuring the O_2 concentration in the electrolyte, Fig. 17), whereas the photogenerated electrons migrate to the substrate through the electrode film. The photocurrent response was stable and reproducible after several illumination cycles and upon several hours of illumination. The photocurrents were remarkably higher than that recorded for a commercial wood-based carbon used for comparison, with current densities up to 0.45 mA/cm^2 for the highest potentials. Even if the reported photocurrent might not be among the highest reported for other water splitting photocatalysts, they were most outstanding for metal-free nanoporous carbon photoanodes. The surface functionalization of the carbon seemed to be an important factor for the performance of the material. Indeed, the faradaic efficiency at short illumination periods was quite small (although increased upon irradiation reaching values close to 90%), indicating that the charge is also consumed in side reactions in the first stages.

The characterization of the photoanodes after illumination corroborated the photo- and electrocorrosion of the anodes due to the occurrence of redox reactions involving the O-, N-, and S-surface groups of the carbon matrix [50,179]; this gives rise to the consumption of the (photo)active sites of the nanoporous carbons and to charge transfer limitations in the photoanodes. The ability of the carbons to oxidize water was linked to the presence of conductive graphene units and "photosensitizers" in these carbons [50]. Light exposure causes the photogeneration of charge carriers on the chromophore-like moieties (ca. sulfone/sulfoxides and some other O- and N-containing groups) whose electrons are excited by irradiation leaving reactive vacancies (holes) able to accept electrons from oxygen in water molecules (in a similar way reported for the visible-light activity of some organic compounds) [160,180]. The conductivity of the carbon matrix and the presence of a well developed porosity are also essential, the latter making the difference between these carbon anodes and graphene or car-

bon nanotubes. The first one facilitates the electron transfer, while the porosity favors the adsorption of water molecules (ca. 18 wt.% for the most performing carbon) in the pores close to the chromophores, thereby enhancing the electron transfer from oxygen to the vacancy.

To further investigate the role of the heteroatoms of the carbon material, and due to the complex surface chemistry of the anodes synthesized from the organic polymer precursor, a series of anodes were prepared from a commodity activated carbon of low functionalization that was chemically modified by wet oxidation and thermal treatment to obtain anodes with different O-moieties [49,174] (Fig. 17).

The photocurrent transients showed the characteristic rectangular shape with the onset potential at about 0.6 V vs Ag/AgCl and currents as high as 0.5 mA/cm^2 for 1 V where the OER was more efficient (extensive bubbling was seen on the electrode surface, not observed in the dark or during the irradiation of the bare collector at the same bias potential). In some electrodes the initial anodic increase upon illumination was preceded by a cathodic current (undershoot), followed by steady-state regime and an equally large anodic overshoot when the illumination was turned-off. Anodic and cathodic current shoots are frequently reported for semiconductors and are attributed to surface recombination processes, photocorrosion phenomena, charge transfer limitations or simultaneous redox reactions occurring at the electrode interface (such as the reduction of O_2 and/or hydroxyl radicals) [121,181]. In our case, the shoots are most likely due to recombination losses upon surface accumulation of holes and electrons at the surface and in the bulk [121], indicating carrier transport limitations and a poorly efficient reaction [122,182]. This was consistent with the low electron mobility of the nanoporous carbons (DC conductivity ranging from 0.5 to 0.02 mS cm^{-1}).

Interestingly, the photocurrent densities of the oxidized carbon electrodes were lower than those of the pristine carbon [49,174]. This contrasts with the performance of the polymer-derived carbons, and indicates that the ability of those anodes was preferentially linked to the presence of S- and N-containing groups,
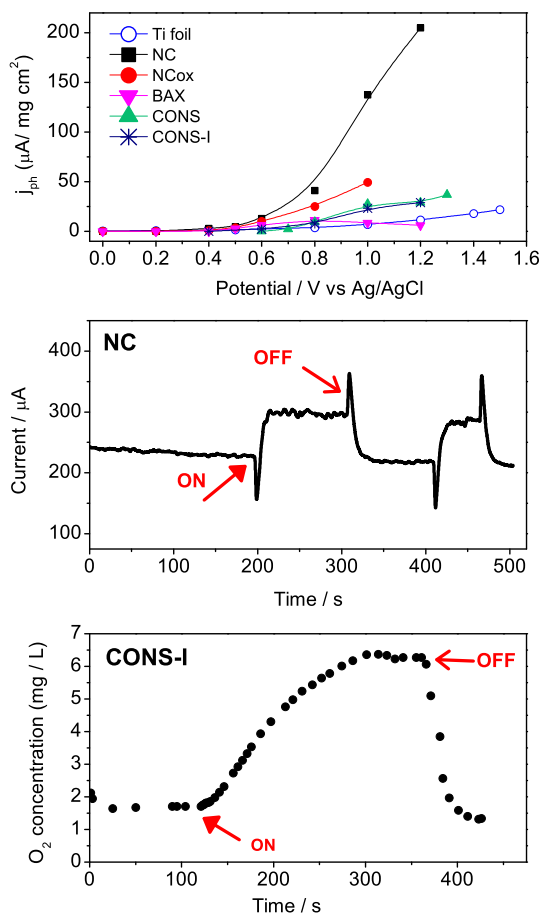
Fig. 17. (top) Photocurrent vs bias potential of nanoporous carbons photoanodes exposed to simulated solar light; (middle) chronoamperometric response of carbon NC photoanode upon on/off illumination at +1 V vs Ag/AgCl, showing the square shaped profile and the cathodic/anodic shoots; (down) Oxygen evolution during the chronoamperometric runs of sample CONS-I. Reprinted from Ref. [50], copyright 2014, with permission from Elsevier.

rather than to the O-functionalities [50]. More importantly, the fact that the as-received carbon showed the highest photocurrent, despite its low surface functionalization (ca. 1.9 wt.% oxygen, with no S- or N-containing groups), gives a new perspective to the origin of the photochemical activity of nanoporous carbons and on the role of the surface chemistry. Firstly, the porosity of this series of photoanodes was quite similar among them and much more developed than those of the polymer-derived carbon referred above (with larger pore volumes adapted for the adsorption of water). Besides porosity, the surface hydrophobicity of the carbons is also important as it determines the wettability (rate and amount of water adsorbed). The oxidized carbons clearly adsorb more water that the pristine one (values of 25, 23, 20 wt.% starting for the oxidized carbon to the as-received one), although all of them presented water adsorption capacities higher than that of the above-mentioned polymer-derived carbon (ca. 18 wt.%). Additionally, oxidation of the carbons affects the stabilization/splitting of the exciton by charge propagation through the carbon matrix (O-groups have a high electron-withdrawing effect on the π electron density of the basal planes), which results in higher surface recombination (i.e., lower photocurrents). The superior electron mobility in the pristine carbon compared to the oxidized counterparts was confirmed by the DC conductivity values. Our previous studies also disregarded the contribution of metal impurities to the photoactivity of this nanoporous carbon [45].

In sum, the photoactivity of the nanoporous carbon with low functionalization for water splitting is certainly not linked to the presence of chromophoric surface groups. Beyond surface wetting and conductivity, the carbon must have photoactive sites inside the pores at which carbon/light/water interactions can take place. Such photorreactive sites would be located at the edges of the basal planes, either associated with surface functionalities or to free edges sites linked to various configurations (carbyne-like and carbene-type) [155,183,184]. The free sites are also responsible for the reactivity of carbons to incorporate heteroatoms to give rise to stable surface functionalities. Hence, the reduced photoactivity of the oxidized carbons would be linked to a lower density of free reactive sites (where the O-groups are incorporated).

3.3. Photorreduction reactions

Most research on the photochemistry of nanoporous carbons has focused so far on exploring the potentialities of these materials to promote oxidation reactions upon illumination, based on their capacity to generate radicals when exposed to light in the presence of water and to catalyze the splitting of water [45–50,157,185]. On the other hand, the ability of functionalized graphene materials as electrocatalysts in the ORR [50,186–190] has also been extensively investigated; the ability of the graphene-like materials to boost reduction reactions has been explained due to the changes in the charge distribution in the carbon atoms close to N- and S-groups [191–193]. Following this idea, we have analyzed the capacity of nanoporous carbons to catalyze reduction reactions, either direct photoreductions by the electrons ejected from the carbon matrix exposed to light, or indirect reactions involving other reactive and/or intermediate species.

We have observed that the carbon surface functionalization seems to be a key factor to promote such reductions reactions [50,174], as in many cases the absorption of photons by the carbon matrix can cause modifications in the carbon's surface (Fig. 18). For highly functionalized nanoporous carbons (N- and S-functionalized) that displayed photochemical activity to catalyze the splitting of water, it was found that the photogenerated electrons reduced the surface moieties of the carbon. Several complementary techniques (including XPS for surface characterization, changes in the electrochemical response of the carbon electrodes and the hydrophobicity of the carbon electrode) confirmed the reduction of surface groups (i.e., quaternary nitrogen to pyridinic configurations, carboxylic acid groups, sulfonic acids, and sulfones) upon illumination under UV and visible light [50,194]. The strong surface reducing effect upon light exposure was linked to the affinity of the carbons to adsorb water, as essential mechanism in the efficient electron transfer from water to the vacancies of the chromophore groups of the carbons. This in an important finding as it explains why the photoactivity of certain nanoporous carbons can be largely reduced after long illumination periods, thereby decreasing the efficiency of the material as photo- or electrocatalyst [50,174].

Besides being used for the reduction of some groups in the carbon's surface, the photogenerated electrons may also contribute to some other reduction reactions. Some evidences have been found for the reduction of oxygen and methylviologen. The activity of S-, N-functionalized nanoporous carbons to promote the photoassisted ORR was suspected based on the light-driven enhanced capacitive behavior of carbon electrodes exposed to visible light in acidic (sulfuric) medium [195]. The increased capacitance upon illumination of the electrodes was linked to the oxidation of the carbon surface by photogenerated active radicals, which would make more pores accessible to the charge storage. The effect was not observed in neutral electrolyte, or when oxygen was not present in the system.
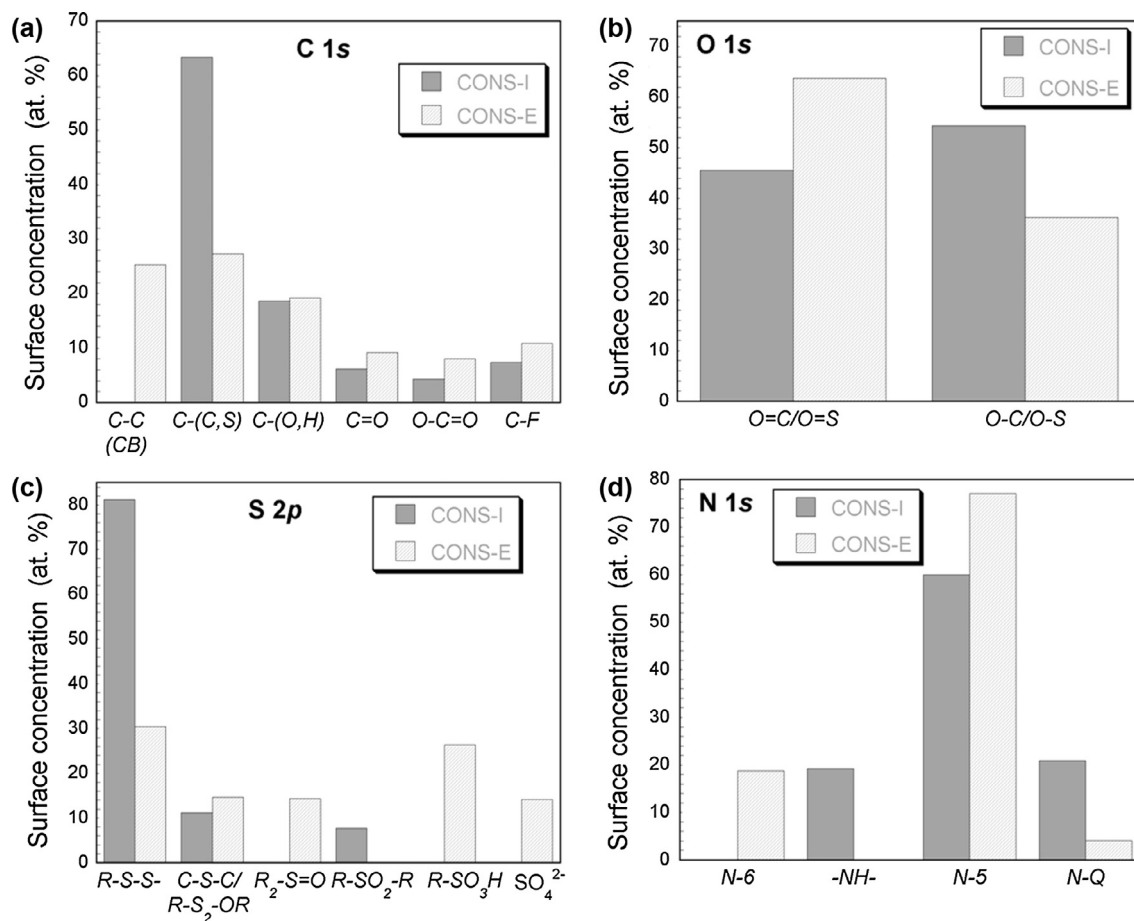
Fig. 18. Surface concentration (at.%) of carbon, oxygen, sulfur and nitrogen species obtained by fitting the C 1s, O 1s, S 2p and N 1s core level peaks of XPS spectra. Reprinted from Ref. [50], copyright 2014, with permission from Elsevier.

On the other hand, we have recently observed the photocatalytic reduction of cationic methylviologen (MV^{2+}) upon irradiation of nanoporous carbons of low functionalization using pulses of a laser flash in the absence of oxygen [196]. Methylviologen molecules act as acceptors of the photogenerated electrons formed in the nanoporous carbon, favoring the interfacial charge transfer and hence the exploitation of the exciton in photocatalytic process. Furthermore, the use of flash photolysis allowed to measure the transient species when an aqueous suspension of nanoporous carbon is irradiated by a laser flash, pointing out the formation of excited species when light interacts with these carbon materials, despite their low functionalization. The identification of these species still remains under investigation.

3.4. Photoluminescent properties of nanoporous carbons

Another field that has growth in recent times is the exploration of the photoluminescent properties of carbon materials, due to their exciting applications in emerging scientific and technological disciplines such as bioimaging, biosensing, photonics, energy storage and conversion, drug delivery, and optoelectronics. Many efforts have been devoted to the exploration of carbon nanotubes, graphene-like materials, and particularly carbon dots, as they can be easily prepared by a various approaches and precursors, which allows a precise band gap control that defines their optoelectronic properties for emerging quantum technologies [185,197–200]. The interest for nanoporous carbon materials (beyond carbon

nanotubes) has not been so successful [185], despite the fact the mechanisms postulated for understanding the origin of the photoactivity of nanoporous carbons (see above sections) are quite similar to those proposed for the photoluminescence of non-porous carbons (e.g., the presence of sp^2 clusters capable of the localization of electron-hole pair followed by their radiative recombination in nearby localized electronic states [197,198], the existence of fluorophores and chromophores on the surface of the carbons, specific electron transition between functionalized carbon atom regions, and crosslink-enhanced emission effects) [199].

Some works have explored the use of carbon materials with certain porosity such as nanotubes, nanofibers and nanocoils [200] as well as nanostructured amorphous carbon films [201,202], showing varied photoluminescence features (i.e., absorption and emission peaks at different wavelengths including the visible range), that have mainly been linked to the electronic features of the materials and their dispersion/aggregation state.

More recently, Bandosz et al. reported the photoluminescence of nanoporous carbons rich in photosensitizes (N-, S- and O-heteroatoms) in water and *n*-propanol [203]. A photoluminescence signal was observed despite the strong light absorbing nature of these carbons, and was linked to the complex surface chemistry (sulfones, sulfoxides, sulfonic acids and *N*-groups acting as chromophores) and high electrical conductivity of those carbons, the latter provided by the presence of conductive graphene domains. What is importantly demonstrated in this work is that the

nanoporosity of the carbons is also critical; in this regard, photoluminescence assays carried out in various solvents (to block the porosity of the carbons via adsorption) demonstrated that when the pores are filled with a solvent, there is a marked decrease in the luminescence signal in water [203].

4. Conclusions

The use of nanoporous carbons in photochemical reactions-covering their role as additives to semiconductors and as photocatalysts themselves-, has become an interesting topic that has opened new opportunities for these materials in various disciplines related to light harvesting and applied photochemistry in nanoconfined systems. In their role of additives to semiconductors, intensive research has been carried out coupling different forms of nanoporous carbons to TiO$_2$ as well as to other semiconductors, in an attempt to overcome the major technological limitation of these materials related to their low photonic efficiency under sunlight. While many studies have reported the superior performance of semiconductor/nanoporous carbon composites under solar irradiation, particularly by the use of new semiconductors based on mixed metal oxides (e.g., bismuth and tungsten-derived) with improved absorption features in the visible range, our studies have demonstrated the key role of the choice of the carbon additive, and the route for the synthesis of the semiconductor/carbon photocatalysts. Besides the light harvesting features of the photocatalyst, it becomes crucial to optimize the interfacial interactions between the target molecule and the catalyst's surface so as to attain a perfect semiconductor/carbon/molecule coupling. Hence, a nanoporous carbon additive performing nicely for a given semiconductor, may not give optimum results when used as additive to a different semiconductor and/or in a different reaction where the interactions between the catalysts surface and the target molecule may not be favorable.

On the other hand, despite the singular and promising optical features of graphene and carbon nanotubes have been known for some time and intensively investigated, research on exploring the photochemical properties of nanoporous carbons has not received much attention (despite the close similarities between the structural and chemical features of nanoporous carbons and those of graphene). Indeed, while a few studies have reported evidences on the photoactivity of carbon nanotubes and graphene-based nanocomposites under varied illumination conditions (including sunlight) [123–125], knowledge on nanoporous carbon/semiconductor photochemistry has been traditionally associated to the role of carbons as non-photoactive porous supports [30,67]. In 2010 we provided the proof of the concept for the photochemical activity of semiconductor-free nanoporous carbons under UV–visible irradiation through their ability to promote the photooxidation of aromatic pollutants in solution, as well as to photogenerate reactive radical species when irradiated in aqueous environments [42–45]. Aiming at understanding this behavior and the mechanisms governing the photochemical activity of nanoporous carbons, we continued this research line exploring the possibilities in various fields of application, covering the photooxidation of pollutants of different chemical structure in water [42,43,126], as well as the use of nanoporous carbon photoanodes in the water photooxidation reaction, and in photorreduction reactions. For this purpose, we designed a novel approach consisting on irradiating the materials preloaded with the target molecule adsorbed inside the porosity of the catalyst. This allowed the evaluation of the photochemical quantum yield of the reactions in the confined pore voids of the carbons, while avoiding secondary parasitic processes (adsorption, photolysis) that occur simultaneously on nanoporous

materials, and that make difficult the accurate determination of the quantum efficiency and turnover using nanoporous catalysts.

The dual nature of nanoporous carbons with ad-hoc designed pore architectures acting as nanoreactors (confinement) and photoactivity that may be modulated by modifying the chemical composition of the carbon, offers new perspectives in the fields of light conversion. Conceptually, the potentialities of the photochemical activity of nanoporous carbons have been demonstrated for various reactions mainly in aqueous environments, with carbons showing ability to photogenerate oxygen-based radical species when exposed to UV or sunlight. Limitations, however, relate to their low photochemical quantum yields (yet to be improved by mastering the synthesis of these materials), and limited stability under long illumination periods due to surface photocorrosion. Particularly much progress has been made in the photocatalytic degradation of pollutants using semiconductor/carbon and nanoporous carbons as catalysts, where the possibilities of the photochemical properties of nanoporous carbons coupled to highly skilled adsorption technologies could settle the basis for a short-term implementation of carbon-based advanced oxidation processes for water treatment and air purification.

On the other hand, some progress is yet to be done towards the understanding of the fundamentals of the photochemical and photophysical properties of nanoporous carbons and the light/carbon/molecule interactions at a nanoscale level, as the key for integrating photochemical reactions based on semiconductor-free nanoporous carbons in a wide panel of technological processes. In this regard, porosity is a critical parameter since it controls the kinetics of the photoassisted reaction (thus, the overall efficiency); the tight nanoconfinement inside the pores is also important since the proximity between the photogenerated charge carriers and the adsorbed molecule in the constrained nanopore space facilitates the exciton splitting and charge separation, minimizing surface recombination. Matching of the molecular dimensions of the target compound confined in the carbon porous network has also been reported to boost the exploitation of light towards the visible spectrum, with about 100 nm red-shift.

Surface functionalization of the nanoporous carbon is also important, as it might affect the electron-acceptor capacity of the carbon matrix (thus delocalization of the exciton); some surface groups (chromophoric moieties) might become excited upon light absorption, enhancing the photochemical quantum yield of nanoporous carbons as multiphase systems.

The dependence of the photochemical activity of nanoporous carbons on the pore confinement and surface chemistry herein described is expected to be valuable in general for targeting other applications in the fields of solar energy conversion (e.g. water splitting, carbon photofixation reactions, photovoltaic devices). The challenge on the use of sustainable metal-free carbon photocatalysts with enhanced response under solar light is yet to design carbons with optimized tailor-made features at different levels: multimodal pore control at the nanometric level, surface functionalization with chromophoric photoactive groups with enhanced response under solar irradiation, and high electron mobility.

References

[1] P.V. Kamat, Emergence of new materials for light-energy conversion: perovskites, J. Phys. Chem. Lett. 5 (2014) 4167–4168.
[2] M.M. Lee, J. Teuscher, T. Miyasaka, T.N. Murakami, H.J. Snaith, Efficient hybrid solar cells based on meso-superstructured organometal halide perovskites, Sci. Mag. 338 (2012) 643–647.
[3] M.A. Green, A. Ho-Baillie, H.J. Snaith, The emergence of perovskite solar cells, Nat. Photonics 8 (2014) 506–514.
[4] S.D. Stranks, H.J. Snaith, Metal-halide perovskites for photovoltaic and light-emitting devices, Nat. Nanotechnol. 10 (2015) 391–402.
[5] O. Malinkiewicz, A. Yella, Y.H. Lee, G. Mínguez-Espallargas, M. Graetrel, M.K. Nazeeruddin, H.J. Bolink, Perovskite solar cells employing organic charge-transport layers, Nat. Photonics 8 (2014) 28–132.
[6] S.G. Kumar, K.S.R.K. Rao, Tungsten-based nanomaterials (WO$_3$ & Bi$_2$WO$_6$): modifications related to charge carrier transfer mechanisms and photocatalytic, Appl. Surf. Sci. 355 (2015) 939–958.
[7] J.W. Tang, Z.G. Zou, J.H. Ye, Efficient photocatalytic decomposition of organic contaminants over CaBi$_2$O$_4$ under visible-light irradiation, Angew Chem. Int. Ed. 43 (2004) 4463–4466.
[8] W. Guosheng, N. Tomohiro, O. Bunsho, C. Aicheng, Synthesis and characterization of carbon-doped TiO$_2$ nanostructures with enhanced visible light response, Chem. Mater. 19 (2007) 4530–4537.
[9] J.C. Yu, W. Ho, J. Yu, H. Yip, P.K. Wong, J. Zhao, Efficient visible-light-induced photocatalytic disinfection on sulfur-doped nanocrystalline titania, Environ. Sci. Technol. 39 (2005) 1175–1179.
[10] M.I. Litter, J.A. Navio, Photocatalytic properties of iron-doped titania semiconductors, J. Photochem. Photobiol. A Chem. 98 (1996) 171–181.
[11] F. Han, V.S.R. Kambala, M. Srinivasan, D. Rajarathnam, R. Naidu, Tailored titanium dioxide photocatalysts for the degradation of organic dyes in wastewater treatment: a review, Appl. Catal. A 359 (2009) 25–40.
[12] C. Minero, G. Mariella, V. Maurino, E. Pelizzetti, Photocatalytic transformation of organic compounds in the presence of inorganic anions. 1. Hydroxyl-mediated and direct electron-transfer reactions of phenol on a titanium dioxide-fluoride system, Langmuir 16 (2000) 2632–2641.
[13] K. Lv, X. Li, K. Deng, J. Sun, X. Li, M. Li, Effect of phase structures on the photocatalytic activity of surface fluorinated TiO$_2$, Appl. Catal. B – Environ. 95 (2010) 383–392.
[14] E.M. Rockafellow, L.K. Stewart, W.S. Jenks, Is sulfur-doped TiO$_2$ an effective visible light photocatalyst for remediation?, Appl Catal. B – Environ. 91 (2009) 554–562.
[15] S.U.M. Khan, M. Al-Shahry, W.B. Ingler Jr, Efficient photochemical water splitting by a chemically modified n-TiO$_2$, Science 297 (2002) 2243–2245.
[16] R. Asahi, T. Morikawa, T. Ohwaki, K. Aoki, Y. Taga, Visible-light photocatalysis in nitrogen-doped titanium oxides, Science 293 (2001) 269–271.
[17] S. Sakthivel, H. Kisch, Daylight photocatalysis by carbon-modified titanium dioxide, Angew. Chem. Int. Edit. 42 (2003) 4908–4911.
[18] S. Sakthivel, M. Janczarek, H.J. Kisch, Visible light activity and photoelectrochemical properties of nitrogen-doped TiO$_2$, Phys. Chem. B 108 (2004) 19384–19387.
[19] Y. Cho, W. Choi, C.H. Lee, T. Hyeon, H.I. Lee, Visible light-induced degradation of carbon tetrachloride on dye-sensitized TiO$_2$, Environ. Sci. Technol. 35 (2001) 966–970.
[20] E. Bae, W. Choi, Highly enhanced photoreductive degradation of perchlorinated compounds on dye-sensitized metal/TiO$_2$ under visible light, Environ. Sci. Technol. 37 (2002) 147–152.
[21] J. Maçaira, L. Andrade, A. Mendes, Review on nanostructured photoelectrodes for next generation dye-sensitized solar cells, Renew. Sust. Energy Rev. 27 (2013) 334–349.
[22] W. Luo, R. Yul, Y. Wang, Z. Li, J. Ye, Z. Zou, Enhanced photocurrent–voltage characteristics of WO$_3$/Fe$_2$O$_3$ nano-electrodes, J. Phys. D: Appl. Phys. 40 (2007) 1091–1096.
[23] A. Cordero-García, J.L. Guzmán-Mar, L. Hinojosa-Reyes, E. Ruiz-Ruiz, A. Hernández-Ramírez, Effect of carbon doping on WO$_3$/TiO$_2$ coupled oxide and its photocatalytic activity on diclofenac degradation, Ceram. Int. 42 (2016) 9796–9803.
[24] H. Choi, E. Stathatos, D. Dionysiou, Sol-gel preparation ofmesoporous photocatalytic TiO$_2$ films and TiO$_2$/Al$_2$O$_3$ composite membranes for environmental applications, Appl. Catal. B – Environ. 63 (2006) 60–67.
[25] A. Fernández, G. Lassaletta, V.M. Jiménez, A. Justo, A.R. González-Elipe, J.M. Herrmann, H. Tahirin, Y. Ait-Ichou, Preparation and characterization of TiO$_2$ photocatalysts supported on various rigid supports (glass, quartz and stainless steel). Comparative studies of photocatalytic activity in water purification, Appl. Catal. B – Environ. 7 (1995) 49–63.
[26] R. Leary, A. Westwood, Carbonaceous nanomaterials for the enhancement of TiO$_2$ photocatalysis, Carbon 49 (2011) 741–772.
[27] V. Etacheria, C. Di Valentinc, J. Schneiderd, D. Bahnemannd, S.C. Pillai, Visible-light activation of TiO$_2$ photocatalysts: advances in theory and experiments, J. Photoch. Photobio. C 25 (2015) 1–29.
[28] S. Cao, J. Yu, Carbon-based H$_2$-production photocatalytic materials, J. Photoch. Photobio. C 27 (2016) 72–99.
[29] J.L. Faria, W. Wang, Carbon Materials for Catalysis, Chapter 13, John Wiley & Sons, New York, 2009.
[30] J. Matos, J. Laine, J.M. Herrmann, Synergy effect in the photocatalytic degradation of phenol on a suspended mixture of titania and activated carbon, Appl. Catal. B –Environ. 18 (1998) 281–291.
[31] X.H. Xia, Z.H. Jia, Y. Yu, Y. Liang, Z. Wang, L.L. Ma, Preparation of multi-walled carbon nanotube supported TiO$_2$ and its photocatalytic activity in the reduction of CO$_2$ with H$_2$O, Carbon 45 (2007) 717–721.
[32] H.T. Yu, X. Quan, S. Chen, H. Zhao, TiO$_2$-multiwalled carbon nanotube heterojunction arrays and their charge separation capability, J. Phys. Chem. C 35 (2007) 12987–12991.
[33] S. Stankovich, D.A. Dikin, G.H.B. Dommett, K.M. Kohlhaas, E.J. Zimney, E.A. Stach, R.D. Piner, S.T. Nguyen, R.S. Ruoff, Graphene-based composite materials, Nature 442 (2006) 282–286.
[34] G. Williams, B. Seger, P.V. Kamat, TiO$_2$-graphene nanocomposites. UV-assisted photocatalytic reduction of graphene oxide, ACS Nano 2 (2008) 1487–1491.
[35] Y. Zhang, Z.R. Tang, X. Fu, Y.J. Xu, TiO$_2$–graphene nanocomposites for gas-phase photocatalytic degradation of volatile aromatic pollutant: is TiO$_2$-graphene truly different from other TiO$_2$-carbon composite materials?, ACS Nano 4 (2010) 7303–7314.
[36] H. Zhang, X. Lv, Y. Li, Y. Wang, J. Li, P25-graphene composite as a high performance photocatalyst, ACS Nano 4 (2010) 380–386.
[37] S. Wang, D. Choi, J. Li, Z. Yang, Z. Nie, R. Kou, D. Hu, C. Wang, L.F. Saraf, J. Zhang, I.A. Aksay, J. Liu, Self-assembled TiO$_2$-graphene hybrid nanostructures for enhanced Li-ion insertion, ACS Nano 3 (2009) 907–991.
[38] K. Woan, G. Pyrgiotakis, W. Sigmund, Photocatalytic carbon-nanotube–TiO$_2$ composites, Adv. Mater. 21 (2009) 2233–2239.
[39] W. Wang, P. Serp, P. Kalck, J.L. Faria, Visible light photodegradation of phenol on MWNT-TiO$_2$ composite catalysts prepared by a modified sol-gel method, J. Mol. Catal. A Chem. 235 (2005) 194–199.
[40] X. Wang, Z. Hu, Y. Chen, G. Zhao, Y. Liu, Z. Wen, A novel approach towards high-performance composite photocatalyst of TiO$_2$ deposited on activated carbon, Appl. Surf. Sci. 255 (7) (2009) 3953–3958.
[41] R. Ocampo-Pérez, M. Sánchez-Polo, J. Rivera-Utrilla, R. Leyva-Ramos, Enhancement of the catalytic activity of TiO$_2$ by using activated carbon in the photocatalytic degradation of cytarabine, Appl. Catal. B – Environ. 104 (2011) 177–184.
[42] L.F. Velasco, J.B. Parra, C.O. Ania, Role of activated carbon features on the photocatalytic degradation of phenol, Appl. Surf. Sci. 256 (2010) 5254–5258.
[43] L.F. Velasco, I.M. Fonseca, J.B. Parra, J.C. Lima, C.O. Ania, Photochemical behaviour of activated carbons under UV irradiation, Carbon 50 (2012) 249–258.
[44] L.F. Velasco, E. Maurino, E. Laurenti, C.O. Ania, Spectroscopic evidence of light-induced generation of radicals on carbon materials, Appl. Catal. A – Gen. 453 (2013) 310–315.
[45] L.F. Velasco, E. Maurino, E. Laurenti, I.M. Fonseca, J.C. Lima, C.O. Ania, Photoinduced reactions occurring on activated carbons. A combined photooxidation and ESR study, Appl. Catal. A – Gen. 452 (2013) 1–8.
[46] L.F. Velasco, J.C. Lima, C.O. Ania, Visible-light photochemical activity of nanoporous carbons under monochromatic light, Angew. Chem. Int. Ed. 53 (2014) 4146–4148.
[47] L.F. Velasco, R.J. Carmona, J. Matos, C.O. Ania, Performance of activated carbons in consecutive phenol photooxidation cycles, Carbon 73 (2014) 206–215.
[48] A. Gomis-Berenguer, M. Seredych, J.C. Lima, J. Iniesta, T.J. Bandosz, C.O. Ania, Sulfur-mediated photochemical energy harvesting in nanoporous carbons, Carbon 104 (2016) 253–259.
[49] L.F. Velasco, A. Gomis-Berenguer, J.C. Lima, C.O. Ania, Tuning the surface chemistry of nanoporous carbons for an enhanced nanoconfined photochemical activity, ChemCatChem 7 (2015) 3012–3319.
[50] C.O. Ania, S. Seredych, E. Rodríguez-Castellón, T.J. Bandosz, Visible light driven photoelectrochemical water splitting on metal free nanoporous carbon promoted by chromophoric functional groups, Carbon 79 (2014) 432–441.
[51] T.I. Barry, F.S. Stone, The reactions of oxygen at dark and irradiated zinc oxide surface, Proc. Royal Soc. 255 (1960) 124–144.
[52] A. Fujishima, K. Honda, Electrochemical photolysis of water at a semiconductor electrode, Nature 238 (1972) 37–38.
[53] A. Kudo, K. Ueda, H. Kato, I. Mikami, Photocatalytic O$_2$ evolution under visible light irradiation on BiVO$_4$ in aqueous AgNO$_3$ solution, Catal. Lett. 53 (1998) 229–230.
[54] A. Kudo, S. Hijii, H$_2$ or O$_2$ evolution from aqueous solutions on layered oxide photocatalysts consisting of Bi^{3+} with 6s^2 configuration and d^0 transition metal ions, Chem. Lett. 28 (1999) 1103–1104.
[55] M. Long, W. Cai, J. Cai, B. Zhou, X. Chai, Y. Wu, Efficient photocatalytic degradation of phenol over Co$_3$O$_4$/BiVO$_4$ composite under visible light irradiation, J. Phys. Chem. B 110 (2006) 20211–20216.
[56] D.K. Lee, I.S. Cho, S. Lee, S.T. Bae, J.H. Noh, D.W. Kim, K.S. Hong, Effects of carbon content on the photocatalytic activity of C/BiVO$_4$ composites under visible light irradiation, Mater. Chem. Phys. 119 (2010) 106–111.
[57] A. Fujishima, T.N. Rao, D.A. Tryk, Titanium dioxide photocatalysis, J. Photochem. Photobiol. C Photochem. Rev. 1 (2000) 1–21.
[58] M.A. Henderson, A surface science perspective on TiO$_2$ photocatalysis, Surf. Sci. Rep. 66 (2011) 185–297.
[59] N. Serpone, E. Pelizzetti, Photocatalysis: Fundamental and Applications, Wiley Interscience, New York, 1989.

[60] J.M. Herrmann, Heterogeneous photocatalysis: fundamentals and applications to the removal of various types of aqueous pollutants, Catal. Today 53 (1999) 115–129.

[61] A. Kudo, Y. Miseki, Heterogeneous photocatalyst materials for water splitting, Chem. Soc. Rev. 38 (2009) 253–278.

[62] X. Hu, G. Li, J.C. Yu, Design, fabrication, and modification of nanostructured semiconductor materials for environmental and energy applications, Langmuir 26 (2009) 3031–3039.

[63] J.C. Yu, J.J. Yu, W. Ho, L. Zhang, Preparation of highly photocatalytic active nano-sized TiO_2 particles via ultrasonic irradiation, Chem. Commun. (2001) 1942–1943.

[64] W. Ho, J.C. Yu, S. Lee, Low-temperature hydrothermal synthesis of S-doped TiO_2 with visible light photocatalytic activity, J. Solid State Chem. 179 (2006) 1171–1176.

[65] E. Pelizzetti, N. Serpone, Photocatalysis: Fundamental and Applications, Wiley, New York, 1989.

[66] M. Pelaez, N.T. Nolan, S.C. Pillai, M.K. Seery, P. Falaras, A.G. Kontos, P.S.M. Dunlop, J.W.J. Hamilton, J.A. Byrne, K. O'Shea, M.H. Entezari, D.D. Dionysiou, A Review on the visible light active titanium dioxide photocatalysts for environmental applications, Appl. Catal. B – Environ. 125 (2012) 331–349.

[67] B. Tryba, Increase of the photocatalytic activity of TiO_2 by carbon and iron modifications, J. Photoenergy. 2008; ID 721824, p. 1–15.

[68] X. Zhang, M. Zhou, L. Lei, Preparation of photocatalytic TiO_2 coatings of nanosized particles on activated carbon by APMOCVD, Carbon 438 (2005) 1700–1708.

[69] J. Matos, J. Laine, J.M. Herrmann, Effect of the type of activated carbons on the photocatalytic degradation of aqueous organic pollutants by UV-irradiated titania, J. Catal. 200 (2001) 10–20.

[70] J. Araña, J.M. Doña-Rodríguez, E. Tello Rendón, C. Garriga i Cabo, O. González-Díaz, J.A. Herrera-Melián, J. Pérez-Peña, G. Colón, J.A. Navío, TiO_2 activation by using activated carbon as a support: Part II. Photoreactivity and FTIR study, Appl. Catal. B – Environ. 44 (2003) 153–160.

[71] C. Minero, F. Catozzo, E. Pelizzetti, Role of adsorption in photocatalyzed reactions of organic molecules in aqueous TiO_2 suspensions, Langmuir 8 (1992) 481–486.

[72] B. Tryba, A.W. Morwski, M. Inagaki, Application of TiO_2-mounted activated carbon to the removal of phenol from water, Appl. Catal. B 41 (2003) 427–433.

[73] R.J. Carmona, L.F. Velasco, V. Maurino, E. Laurenti, C.O. Ania, Carbon Materials as additives to WO_3 for an enhanced conversion of simulated solar light, Front. Mater. 3 (2016) 1–11.

[74] J. Matos, A. García, M.M. Titirici, Solvothermal carbon-doped TiO_2 photocatalyst for the enhanced methylene blue degradation under visible light, Appl. Catal. A – Gen. 390 (2010) 175–182.

[75] M. Andrade, A.S. Mestre, R.J. Carmona, A.P. Carvalho, C.O. Ania, Effect of the irradiation wavelength on the performance of nanoporous carbon as an additive to TiO_2, Appl. Catal. A – Gen. 507 (2015) 91–98.

[76] L.F. Velasco, J.B. Parra, C.O. Ania, Phenol adsorption and photo-oxidation on porous carbon/titania composites, Adsorpt. Sci. Technol. 28 (2010) 727–738.

[77] A. Santos, P. Yustos, A. Quintanilla, S. Rodríguez, F. García-Ochoa, Route of the catalytic oxidation of phenol in aqueous phase, Appl. Catal. B – Environ. 39 (2002) 97–113.

[78] C.G. Silva, J.L. Faria, Photocatalytic oxidation of phenolic compounds using carbon nanotube-TiO_2 composite catalyst, ChemSusChem 5 (2010) 609–618.

[79] W. Wang, P. Serp, P. Kalck, C.G. Silva, J.L. Faria, Preparation and characterization of nanostructured MWCNT-TiO_2 composite materials for photocatalytic water treatment application, Mater. Res. Bull. 43 (2008) 958–967.

[80] L.F. Velasco, M. Haro, J. Parmentier, R. Gadiou, C. Vix-Guterl, C.O. Ania. Tuning the photocatalytic activity and optical properties of mesoporous TiO_2 spheres by a carbon scaffold, J. Catal. 2013; Article ID 178512: 1–9.

[81] X.M. Sun, Y.D. Li, Colloidal carbon spheres and their core/shell structures with noble-metal nanoparticles, Angew. Chem. Int. Ed. 43 (2001) 597–601.

[82] W. Shen, Y. Zhu, X. Dong, J. Gu, J. Shi, A new strategy to synthesize TiO_2-hollow spheres using carbon spheres as template, Chem. Lett. 34 (2005) 840–841.

[83] J. Matos, A. García, P.S. Poon, Environmental green chemistry applications of nanoporous carbons, J. Mater. Sci. 45 (2010) 4934–4944.

[84] R.B. Zheng, X.W. Meng, F.Q. Tang, A general protocol to coat titania shell on carbon-based composites cores using carbon as coupling agent, J. Solid State Chem. 182 (2009) 1235–1240.

[85] D.K. Lee, S.C. Kim, S.J. Kim, I.S. Chung, S.W. Kim, Photocatalytic oxidation of microcystin-LR with TiO2-coated activated carbon, Chem. Eng. 2004 (102) (2004) 93–98.

[86] L.F. Velasco, B. Tsyntsarski, B. Petrova, T. Budinova, N. Petrov, J.B. Parra, C.O. Ania, Carbon foams as catalyst supports for phenol photodegradation, J. Hazard. Mater. 184 (2010) 843–848.

[87] M. Haro, L.F. Velasco, C.O. Ania, Carbon-mediated photoinduced reactions as a key factor in the photocatalytic performance of C/TiO_2, Catal. Sci. Technol. 2 (2012) 2264–2272.

[88] B. Llano, G. Restrepo, J.M. Marín, J.A. Navío, M.C. Hidalgo, Characterisation and photocatalytic properties of titania-silica mixed oxides doped with Ag and Pt, Appl. Catal. A – Gen. 387 (2010) 135–140.

[89] W.Y. Choi, A. Termin, M.R. Hoffmann, The role of metal-ion dopants in quantum-sized TiO_2 – correlation between photoreactivity and charge-carrier recombination dynamics, J. Phys. Chem. – Us 98 (1994) 13669–13679.

[90] S.N.R. Inturi, T. Boningari, M. Suidan, P.G. Smirniotis, Visible light-induced photodegradation of gas phase acetonitrile using aerosol-made transition metal (V, Cr, Fe Co, Mn, Mo, Ni, Cu, Y, Ce, and Zr) doped TiO_2, Appl. Catal. B – Environ. 144 (2014) 333–342.

[91] M. Maicu, M.C. Hidalgo, G. Colón, J.A. Navío, Comparative study of the photodeposition of Pt, Au and Pd on pre-sulphated TiO_2 for the photocatalytic decomposition of phenol, J. Photochem. Photobiol. A 217 (2011) 275–283.

[92] M. Andrade, A.S. Mestre, J. Matos, A.P. Carvalho, C.O. Ania, Visible light driven photooxidation of phenol on TiO_2/Cu-loaded carbon catalysts, Carbon 76 (2014) 183–196.

[93] H. Irie, S. Miura, K. Kamiya, K. Hashimoto, Efficient visible light-sensitive photocatalysts: grafting Cu(II) ions onto TiO_2 and WO_3 photocatalysts, Chem. Phys. Lett. 457 (2008) 202–205.

[94] G. Colón, M. Maicu, M.C. Hidalgo, J.A. Navío, Cu-doped TiO_2 systems with improved photocatalytic activity, Appl. Catal. B – Environ. 67 (2006) 41–51.

[95] H. Nishikiori, T. Sato, S. Kubota, N. Tanaka, Y. Shimizu, T. Fujii, Preparation of Cu-doped TiO_2 via refluxing of alkoxide solution and its photocatalytic properties, Res. Chem. Intermed. 38 (2012) 595–613.

[96] R.M. Mohamed, M.M. Mohamed, Copper (II) phthalocyanines immobilized on alumina and encapsulated inside zeolite-X and their applications in photocatalytic degradation of cyanide: a comparative study, Appl. Catal. A – Gen. 340 (2008) 16–24.

[97] G. Colón, S. Murcia López, M.C. Hidalgo, J.A. Navío, Sunlight highly photoactive Bi_2WO_6-TiO_2 heterostructures for rhodamine B degradation, Chem. Commun. 46 (2010) 4809–4811.

[98] J. Yu, J. Xiong, B. Cheng, Y. Yu, J. Wang, Hydrothermal preparation and visible-light photocatalytic activity of Bi2WO6 powders, J. Solid State Chem. 178 (2005) 1968–1972.

[99] C. Zhang, Y.F. Zhu, Synthesis of square Bi_2WO_6 nanoplates as high-activity visiblelight-driven photocatalysts, Chem. Mater. 17 (2005) 3537–3545.

[100] J.W. Tang, Z.G. Zou, J.H. Ye, Photocatalytic decomposition of organic contaminants by Bi_2WO_6 under visible light irradiation, Catal. Lett. 92 (2004) 53–56.

[101] S. Murcia-López, M.C. Hidalgo, J.A. Navío, Role of activated carbon on the increased photocatalytic activity of AC/Bi_2WO_6 coupled materials, Appl. Catal. A – Gen. 466 (2013) 51–59.

[102] Y.Y. Li, J.P. Liu, X.T. Huang, J.G. Yu, Carbon-modified Bi_2WO_6 nanostructures with improved photocatalytic activity under visible light, J. Chem. Soc. Dalton Trans. 39 (2010) 3420–3425.

[103] Y. Cui, L. Huiquan, H. Wenshan, F. Suhua, Z. Liangjun, The effect of carbon content on the structure and photocatalytic activity of nano-Bi_2WO_6 powder, Powder Technol. 247 (2013) 151–160.

[104] X. Qian, D. Yue, Z. Tian, M. Reng, Y. Zhu, M. Kan, T. Zhang, Y. Zhao, Carbon quantum dots decorated Bi_2WO_6 nanocomposite with enhanced photocatalytic oxidation activity for VOCs, Appl. Catal. B – Environ. 193 (2016) 16–21.

[105] R.J. Carmona, L.F. Velasco, M.C. Hidalgo, J.A. Navío, C.O. Ania, Boosting the visible-light photoactivity of Bi_2WO_6 using acidic carbon additives, Appl. Catal. A 505 (2015) 467–477.

[106] E. Galoppini, Linkers for anchoring sensitizers to semiconductor nanoparticles, Coord. Chem. Rev. 248 (2004) 283–1297.

[107] P. Wang, M. Cheng, Z. Zhang, On different photodecomposition behaviors of rhodamine B on laponite and montmorillonite clay under visible light irradiation, J. Saudi Chem. Soc. 18 (2014) 308–316.

[108] H. Fu, C. Pan, W. Yao, Y. Zhu, Visible-light-induced degradation of rhodamine B by nanosized Bi_2WO_6, J. Phys. Chem. B 190 (2005) 22432–22439.

[109] H. Gad, A.A. El-Sayed, Activated carbon from agricultural by-products for the removal of Rhodamine-B from aqueous solution, J. Hazard. Mater. 168 (2009) 1070–1081.

[110] I. López Arbeloa, P. Ruiz Ojeda, Dimeric states of rhodamine B, Chem. Phys. Lett. 87 (1982) 556–560.

[111] J.B. Asbury, E. Hao, Y. Wang, T. Lian, Bridge length-dependent ultrafast electron transfer from Re polypyridyl complexes to nanocrystalline TiO_2 thin films studied by femtosecond infrared spectroscopy, J. Phys. Chem. B 104 (2000) 11957–11964.

[112] J.S.E.M. Svensson, C.G. Granqvist, Electrochromic tungsten oxide films for energy efficient windows, Sol. Energy Mater. 11 (1984) 29–34.

[113] F.A. Cotton, G. Wilkinson, Advances in Organic Chemistry, fifth ed., Wiley, New York, 1988.

[114] C. Guéry, C. Choquet, F. Dujeancourt, J.M. Tarascon, J.C. Lassegues, Infrared and X-ray studies of hydrogen intercalation in different tungsten trioxides and tungsten trioxide hydrates, J. Solid State Electrochem. 1 (1997) 199–207.

[115] Y. Nosaka, S. Takahashi, H. Sakamoto, A.Y. Nosaka, Reaction mechanism of Cu (II)-grafted visible-light responsive TiO_2 and WO_3 photocatalysts studied by means of ESR spectroscopy and chemiluminescence photometry, J. Phys. Chem. C 115 (2011) 21283–21290.

[116] Z. Wen, W. Wu, Z. Liu, H. Zhang, J. Li, J. Chen, Ultrahigh-efficiency photocatalysts based on mesoporous Pt-WO_3 nanohybrids, Phys. Chem. Chem. Phys. 15 (2013) 6773–6778.

[117] C. Moreno-Castilla, Adsorption of organic molecules from aqueous solutions on carbon materials, Carbon 42 (2004) 83–94.

[118] L.F. Velasco, C.O. Ania, Understanding phenol adsorption mechanisms on activated carbons, Adsorption 17 (2011) 247–254.

[119] G.W. Ho, K.J. Chua, D.R. Siow, Metal loaded WO_3 particles for comparative studies of photocatalysis and electrolysis solar hydrogen production, Chem. Eng. J. 18 (2012) 661–666.

A. Gomis-Berenguer et al./Journal of Colloid and Interface Science 490 (2017) 879–901

[120] A. Gomis-Berenguer, V. Celorrio, J. Iniesta, D.J. Fermin, C.O. Ania, Nanoporous carbon/WO₃ anodes for an enhanced water photooxidation, Carbon 108 (2016) 471–479.

[121] L.M. Peter, Dynamic aspects of semiconductor photoelectrochemistry, Chem. Rev. 90 (1990) 753–769.

[122] S. Xiao, H. Chen, Z. Yang, X. Long, Z. Wang, Z. Zhu, Y. Qu, S. Yang, Origin of the different photoelectrochemical performance of mesoporous BiVO₄ photoanodes between the BiVO₄ and the FTO side illumination, J. Phys. Chem. C 119 (2015) 23350–23357.

[123] Y. Luo, Y. Heng, X. Dai, W. Chen, J. Li, Preparation and photocatalytic ability of highly defective carbon nanotubes, J. Solid State Chem. 182 (2009) 2521–2525.

[124] S. Ameen, H.-K. Seo, M.S. Akhtar, H.S. Shin, Novel graphene/polyaniline nanocomposites and its photocatalytic activity toward the degradation of rose Bengal dye, Chem. Eng. J. 210 (2012) 220–228.

[125] S. Chowdhury, R. Balasubramanian, Graphene/semiconductor nanocomposites (GSNs) for heterogeneous photocatalytic decolorization of wastewaters contaminated with synthetic dyes: a review, Appl. Catal. B – Environ. 160–161 (2014) 307–324.

[126] I. Velo-Gala, J.J. López-Peñalver, M. Sánchez-Polo, J. Rivera-Utrilla, Activated carbon as photocatalyst of reactions in aqueous phase, Appl. Catal. B – Environ. 142–143 (2013) 694–704.

[127] J. Matos, J.M. Chovelon, T. Cordero, C. Ferronato, Influence of surface properties of activated carbon on photocatalytic activity of TiO₂ in 4-chlorophenol degradation, Open Environ. Eng. J. 2 (2009) 21–29.

[128] M. Carballa, F. Omil, J.M. Lema, M. Llompart, C. García-Jares, I. Rodríguez, M. Gómez, T. Ternes, Behavior of pharmaceuticals, cosmetics and hormones in a sewage treatment plant, Water Res. 38 (2004) 2918–2926.

[129] J.E. Drewes, P. Fox, M. Jekel, Occurrence of iodinated X-ray contrast media in domestic effluents and their fate during indirect potable reuse, J. Environ. Sci. Health A Tox Hazard. Subst. Environ. Eng. 36 (2001) 1633–1645.

[130] L.J. Fono, E.P. Kolodziej, D.L. Sedlak, Attenuation of wastewater-derived contaminants in an effluent-dominated river, Environ. Sci. Technol. 40 (2006) 7257–7262.

[131] A. Putschew, S. Wischnack, M. Jekel, Occurrence of triiodinated X-ray contrast agents in the aquatic environment. Sci. Total Environ. 255 (2000) 129–134.

[132] T. Ternes, Pharmaceuticals and metabolites as contaminants of the aquatic environment – an overview, Prepr. Ext. Abstr. ACS Natl. Meet. Am. Chem. Soc. 40 (2000) 98–100.

[133] I. Velo-Gala, J.J. López-Peñalver, M. Sánchez-Polo, J. Rivera-Utrilla, Surface modifications of activated carbon by gamma irradiation, Carbon 67 (2014) 236–249.

[134] R. López, R. Gómez, Band-gap energy estimation from diffuse reflectance measurements on sol-gel and commercial TiO₂: a comparative study, J. Sol-Gel Sci. Technol. 61 (2012) 1–7.

[135] L. Escobar-Alarcón, A. Arrieta, E. Camps, S. Muhl, S. Rodil, E. Vigueras-Santiago, An alternative procedure for the determination of the optical band gap and thickness of amorphous carbon nitride thin films, Appl. Surf. Sci. 254 (2007) 412–415.

[136] S. Adhikari, H.R. Aryal, D.C. Ghimire, G. Kalita, M. Umeno, Optical band gap of nitrogenated amorphous carbon thin films synthesized by microwave surface wave plasma CVD, Diamond Relat. Mater. 17 (2008) 1666–1668.

[137] N. Ahmad, N.A. Tahir, M. Rusop, Amorphous carbon thin films deposited by thermal CVD using camphoric carbon as precursor, Adv. Mater. Res. 403–408 (2012) 646–650.

[138] G. Fanchini, S.C. Ray, A. Tagliaferro, Optical properties of disordered carbon-based materials, Surf. Coat Technol. 151–152 (2002) 233–241.

[139] D. Dasgupta, F. Demichelis, C.F. Pirri, A. Tagliaferro, Π bands and gap states from optical absorption and electron-spin resonance studies on amorphous carbon and amorphous hydrogenated carbon films, Phys. Rev. Sect. B 43 (1991) 2131–2135.

[140] G.H. Chan, B. Deng, M. Bertoni, J.R. Ireland, M.C. Hersam, T.O. Mason, Duyne R. P. Van, J.A. Ibers, Syntheses, structures, physical properties, and theoretical studies of CeMxOS (M = Cu, Ag; x∼0.8) and CeAgOS, Inorg. Chem. 45 (2006) 8264–8272.

[141] Y. Yu, J.C. Yu, C.Y. Chan, Y.K. Che, J.C. Zhao, L. Ding, W.K. Ge, P.K. Wong, Enhancement of adsorption and photocatalytic activity of TiO₂ by using carbon nanotubes for the treatment of azo dye, Appl. Catal. B – Environ. 61 (2005) 1–11.

[142] A. Gomis-Berenguer, J. Iniesta, V. Maurino, J.C. Lima, C.O. Ania, Boosting visible light conversion in the confined pore space of nanoporous carbons, Carbon 96 (2016) 98–104.

[143] E. Finkelstein, G.M. Rosen, E. Rauckman, Spin trapping. Kinetics of the reaction of superoxide and hydroxyl radicals with nitrones, J. Arch. Biochem. Biophys. 200 (1980) 1–16.

[144] C. Minero, A. Bedini, V. Maurino, Glycerol as a probe molecule to uncover oxidation mechanism in photocatalysis, Appl. Catal. B – Environ. 128 (2012) 135–143.

[145] I. Velo-Gala, J.J. López-Peñalver, M. Sánchez-Polo, J. Rivera-Utrilla, Analysis of photocatalytic activity in activated carbon during its interaction with UV light and simulated solar radiation, in: Proceedings to the Conference 40th Reunión Ibérica de Adsorción 2016, Évora (Portugal), ISBN: 978-989-8550-34-7.

[146] M. Rodríguez, N. Ben Abderrazik, S. Contreras, E. Chamarro, J. Giménez, S. Esplugas, Iron(III) photoxidation of organic compounds in aqueous solutions, Appl. Catal. B – Environ. 37 (2002) 131–137.

[147] O. Gimeno, M. Carbajo, F.J. Beltrán, F.J. Rivas, Phenol and substituted phenols AOPs remediation, J. Hazard. Mater. B 119 (2005) 99–108.

[148] H. Kušić, N. Koprivanac, A.L. Božić, I. Selanec, Photo-assisted Fenton type processes for the degradation of phenol: a kinetic study, J. Hazard. Mater. B 136 (2006) 632–644.

[149] L.R. Radovic, C. Moreno-Castilla, J. Rivera-Utrilla, Chemistry, Marcel Dekker, New York, Physics of Carbon. Radovic LR, 2000, pp. 227–405.

[150] V.V. Strelko, V.S. Kuts, P.A. Thrower, On the mechanism of possible influence of heteroatoms of nitrogen, boron and phosphorous in a carbon matrix on the catalytic activity of carbons in electron transfer reactions, Carbon 38 (2000) 1499–1524.

[151] J. Robertson, Mechanical properties and coordinations of amorphous carbons, J. Phys. Rev. Lett. 68 (1992) 220–223.

[152] C. Oppedisano, A. Tagliaferro, Relationship between sp² carbon content and E04 optical gap in amorphous carbon-based materials, Appl. Phys. Lett. 75 (1999) 3650–3652.

[153] H. Karoui, F. Chalier, J.P. Fineta, Tordo. DEMPO: an efficient tool for the coupled ESR-spin trapping of alkylperxyl radicals in water, Org. Biomol. Chem. 9 (2011) 1473–2480.

[154] A.D. Modestov, J. Gun, O. Lev, Graphite photoelectrochemistry study of glassy carbon, carbon-fiber and carbon-black electrodes in aqueous electrolytes by photocurrent response, Surf. Sci. 417 (1998) 311–322.

[155] L.R. Radovic, B. Bockrath, On the chemical nature of graphene edges: origin of stability and potential for magnetism in carbon materials, J. Am. Chem. Soc. 127 (2005) 5917–5927.

[156] Y. Zhu, X. Li, A. Cai, Z. Sun, G. Casillas, M.J. Yacaman, R. Verduzco, J.M. Tour, Quantitative analysis of structure and bandgap changes in graphene oxide nanoribbons during thermal annealing, J. Am. Chem. Soc. 134 (2012) 11774–11780.

[157] T.J. Bandosz, J. Matos, M. Seredych, M.S.Z. Islam, R. Alfano, Photoactivity of S-doped nanoporous activated carbons: a new perspective for harvesting solar energy on carbon-based semiconductors, Appl. Catal. A 445–446 (2012) 159–165.

[158] A. Wang, D.D.L. Chung, Dielectric and electrical conduction behavior of carbon paste electrochemical electrodes, with decoupling of carbon, electrolyte and interface contributions, Carbon 72 (2014) 135–151.

[159] A. Wypych, I. Bobowska, M. Tracz, A. Opasinska, S. Kadlubowski, A. Krzywania-Kaliszewska, J. Grobelny, P. Wojciechowski, Dielectric properties and characterisation of titanium dioxide obtained by different chemistry methods, J. Nanomater. (2014) 1–10 (ID124814).

[160] J.E. Beecher, T. Durst, J.M.J. Fréchet, A. Godt, A. Pangborn, D.R. Robello, C.S. Willans, D.J. Williams, New chromophores containing sulfonamide, sulfonate, or sulfoximide groups for second harmonic generation, Adv. Mater. 5 (1993) 632–634.

[161] M. Baca, G.E. Borgstahl, M. Boissinot, P.M. Burke, D.R. Williams, K.A. Slater, E. D. Getzoff, Complete chemical structure of photoactive yellow protein: novel thioester-linked 4-hydroxycinnamyl chromophore and photocycle chemistry, Biochemistry 33 (1994) 143649–143677.

[162] D.G. Nocera, The artificial leaf, Acc. Chem. Res. 45 (2012) 767–776.

[163] A. Gewirth, M. Thorum, Electroreduction of dioxygen for fuel-cell applications: materials and challenges, Inorg. Chem. 49 (2010) 3557–3566.

[164] H. Dau, C. Limberg, T. Reier, M. Risch, S. Roggan, P. Strasser, The mechanism of water oxidation: from electrolysis via homogeneous to biological catalysis, ChemCatChem 2 (2010) 724–761.

[165] D. Wang, T. Hisatomi, T. Takata, C. Pan, M. Katayama, J. Kubota, K. Domen, Core/shell photocatalyst with spatially separated co-catalysts for efficient reduction and oxidation of water, Angew. Chem. Int. Ed. 52 (2013) 11252–112566.

[166] K. Maeda, D. Lu, K. Domen, Direct water splitting into hydrogen and oxygen under visible light by using modified TaON photocatalysts with d0 electronic configuration, Chem. Eur. J. 19 (2013) 4986–4991.

[167] K. Maeda, Direct splitting of pure water into hydrogen and oxygen using rutile titania powder as a photocatalyst, Chem. Commun. 49 (2013) 8404–8406.

[168] T. Ohmori, H. Takahashi, H. Mametsuka, E. Suzuki, Photocatalytic oxygen evolution on α-Fe₂O₃ films using Fe³⁺ ion as a sacrificial oxidizing agent, Phys. Chem. Chem. Phys. 2 (2000) 3519–3522.

[169] M.W. Kanan, D.G. Nocera, In situ formation of an oxygen-evolving catalyst in neutral water containing phosphate and Co²⁺, Science 321 (2008) 1072–1075.

[170] A. Goux, T. Pauporté, D. Lincot, Oxygen reduction reaction on electrodeposited zinc oxide electrodes in KCl solution at 70 °C, Electrochim. Acta 51 (2006) 3168–3172.

[171] J.A. Seabold, K.S. Choi, Effect of a cobalt-based oxygen evolution catalyst on the stability and the selectivity of photo-oxidation reactions of a WO₃ photoanode, Chem. Mater. 23 (2011) 1105–1112.

[172] X. Li, F.C. Walsh, D. Pletcher, Nickel based electrocatalysts for oxygen evolution in high current density, alkaline water electrolysers, Phys. Chem. Chem. Phys. 13 (2011) 1162–1167.

[173] V. Artero, M. Chavarot Kerlidou, M. Fontecave, Splitting water with cobalt, Angew. Chem. Int. Ed. 50 (2011) 7238–7266.

[174] A. Gomis-Berenguer, I. Velo-Gala, E. Rodríguez-Castellón, C.O. Ania, Surface modification of a nanoporous carbon photoanode upon irradiation, Molecules 21 (2016) 1611, http://dx.doi.org/10.3390/molecules21111611.

[175] Y. Zhao, R. Nakamura, K. Kamiya, S. Nakanishi, K. Hashimoto, Nitrogen-doped carbon nanomaterials as non-metal electrocatalysts for water oxidation, Nat. Commun. 4 (2013) 2390–2397.

[176] T.F. Yeh, C.Y. Teng, S.J. Chen, H. Teng, Nitrogen-doped graphene oxide quantum dots as photocatalysts for overall water-splitting under visible light illumination, Adv. Mater. 26 (2014) 3297–3303.

[177] S. Yang, Y. Gong, J. Zhang, L. Zhan, L. Ma, Z. Fang, et al., Exfoliated graphitic carbon nitride nanosheets as efficient catalysts for hydrogen evolution under visible light, Adv. Mater. 25 (2013) 2452–2456.

[178] T.F. Yeh, S.J. Chen, C.S. Yeh, H. Teng, Tuning the electronic structure of graphite oxide through ammonia treatment for photocatalytic generation of H_2 and O_2 from water splitting, J. Phys. Chem. C 117 (2013) 6516–6524.

[179] A.G. Pandolfo, A.F. Hollenkamp, Carbon properties and their role in supercapacitors, J. Power Sour. 157 (2006) 11–27.

[180] G. Jin, Y. Zhang, W. Cheng, Poly(p-aminobenzene sulfonic acid)-modified glassy carbon electrode for simultaneous detection of dopamine and ascorbic acid, Sens. Act. B 107 (2005) 528–534.

[181] J. Rongé, D. Nijs, S. Kerkhofs, K. Masschaele, J.A. Martens, Chronoamperometric study of membrane electrode assembly operation in continuous flow photoelectrochemical water splitting, Phys. Chem. Chem. Phys. 15 (2013) 9315–9325.

[182] P. Leempoel, Ren F. Fan, A.J. Bard, Semiconductor electrodes. 50. Effect of mode of illumination and doping on photochemical behavior of phthalocyanine films, J. Phys. Chem. 87 (1983) 2948–2955.

[183] L.R. Radovic, P.L. Walker, R.G. Jenkins, Importance of carbon active sites in the gasification of coal chars, Fuel 62 (1983) 849–856.

[184] L.R. Radovic, A.F. Silva-Villalobos, A.B. Silva-Tapia, F. Vallejos-Burgos, Oxygen migration on the graphene surface. 1. Origin of epoxide groups, Carbon 49 (2011) 4218–4225.

[185] T.J. Bandosz, Nanoporous carbons: looking beyond their perception as adsorbents, catalyst supports and supercapacitors, Chem. Rec. 16 (2016) 205–218.

[186] J. Liang, Y. Jiao, M. Jaroniec, S.Z. Qiao, Sulfur and nitrogen dual-doped mesoporous graphene electrocatalyst for oxygen reduction with synergistically enhanced performances, Angew. Chem. Int. Ed. 51 (2012) 11496–11500.

[187] Z. Liu, G. Zhang, Z. Lu, X. Jin, Z. Chang, X. Sun, One-step scalable preparation of N-doped nanoporous carbon as a high-performance electrocatalyst for the oxygen reduction reaction, Nano Res. 6 (2013) 293–301.

[188] J. Liang, Y. Zheng, J. Chen, J. Liu, D. Hulicova-Jurcakova, M. Jaroniec, S.Z. Qiao, Facile oxygen reduction on a three-dimensionally ordered macroporous graphitic C_3N_4/Carbon composite electrocatalyst, Angew. Chem. Int. Ed. 51 (2012) 3892–3896.

[189] M. Seredych, E. Rodríguez-Castellón, M.J. Biggs, W. Skinner, T.J. Bandosz, Effect of visible light and electrode wetting on the capacitive performance of S- and N-doped nanoporous carbons: Importance of surface chemistry, Carbon 78 (2014) 540–558.

[190] M. Seredych, E. Rodríguez-Castellón, T.J. Bandosz, Peculiar properties of mesoporous synthetic carbon/graphene phase composites and their effect on supercapacitive performance, ChemSusChem 8 (2015) 1955–1965.

[191] T.Y. Yang, J. Liu, R.F. Zhou, Z.G. Chen, H.Y. Xu, S.Z. Qiao, M. Monteiro, N-doped mesoporous carbon spheres as the oxygen reduction reaction catalysts, J. Mater. Chem. A 2 (2014) 18139–18146.

[192] J. Liang, X. Du, C. Gibson, X.W. Du, S.Z. Qiao, N-doped graphene natively rotted on hierarchical ordered porous carbon for enhanced oxygen reduction, Adv. Mater. 25 (2013) 6226–6231.

[193] J. Liang, Y. Zheng, J. Chen, J. Liu, D. Hulicova-Jurcakova, M. Jaroniec, S.Z. Qiao, Angew. Chem. Int. Ed. 51 (2012) 3892–3896.

[194] M. Seredych, T.J. Bandosz, Effect of the graphene phase presence in nanoporous S-doped carbon on photoactivity in UV and visible light, Appl. Catal. B: – Environ. 147 (2014) 842–850.

[195] K. Sing, M. Seredych, E. Rodríguez-Castellón, T.J. Bandosz, Effect of visible-light exposure and electrolyte oxygen content on capacitance of sulfur-doped carbon, Chem. Electro. Chem. 1 (2014) 565–572.

[196] A. Gomis-Berenguer, J. Iniesta, C.O. Ania, On the possibilities of photochemistry of nanoporous carbons, in: Proceedings to the Conference Beyond Adsorption: New Perspectives and Challenges for Nanoporous Carbons, 2016, New York (New York City).

[197] G. Eda, Y.Y. Lin, C. Mattevi, H. Yamaguchi, H.A. Chen, I.S. Chen, C.W. Chen, M. Chhowalla, Blue photoluminescence from chemically derived graphene oxide, Adv. Mater. 22 (2010) 505–509.

[198] C. Galande, A.D. Mohite, A.V. Naumov, W. Gao, L. Ci, A. Ajayan, H. Gao, A. Srivastava, R.B. Weisman, P.M. Ajayan, Quasi-molecular fluorescence from graphene oxide, Sci. Rep. 1 (85) (2011) 1–5.

[199] H. Vedala, D.C. Sorescu, G.P. Kotchey, A. Star, Chemical sensitivity of graphene edges decorated with metal nanoparticles, Nano Lett. 7 (2011) 2342–2347.

[200] A. Graf, Y. Zakharko, S.P. Schießl, C. Backes, M. Pfohl, B.S. Flavel, J. Zaumseil, Large scale, selective dispersion of long single-walled carbon nanotubes with high photoluminescence quantum yield by shear force mixing, Carbon 105 (2016) 593–599.

[201] M.S. Medeiros, R.D. Mansano, A.P. Mousi, Photoelectric effects of nanostructured amorphous carbon Films, Microelectron. J. 36 (2005) 981–984.

[202] V. Baranauskas, M.C. Tosin, H.J. Ceragioli, J.G. Zhao, A.C. Peterlevitz, S.F. Durrant, Photoluminescent properties of porous carbon films pyrolized on silicon, Phys. Status Solidi 182 (2000) 395–400.

[203] T.J. Bandosz, E. Rodríguez-Castellón, J.M. Montenegro, M. Seredych, Photoluminescence of nanoporous carbons: Opening a new application route for old materials, Carbon 77 (2014) 651–659.